REPORT DOCUMENTATION PAGE

		1b. RESTRICTIVE MARKINGS
...CLASSIFICATION ED		
		3. DISTRIBUTION / AVAILABILITY OF REPORT
AD-A198 372		APPROVED FOR PUBLIC RELEASE: DISTRIBUTION UNLIMITED
4. PERFORMING ORGANIZATION...		5. MONITORING ORGANIZATION REPORT NUMBER(S)
		AFOSR-TR- 88-0779

6a. NAME OF PERFORMING ORGANIZATION	6b. OFFICE SYMBOL (If applicable)	7a. NAME OF MONITORING ORGANIZATION
UNIVERSITY OF MINNESOTA		AFOSR/NA

6c. ADDRESS (City, State, and ZIP Code)	7b. ADDRESS (City, State, and ZIP Code)
AEROSPACE ENGINEERING AND MECHANICS UNIVERSITY OF MINNESOTA MINNEAPOLIS, MN 55455-0129	BUILDING 410 BOLLING AFB DC 20332-6448

8a. NAME OF FUNDING / SPONSORING ORGANIZATION	8b. OFFICE SYMBOL (If applicable)	9. PROCUREMENT INSTRUMENT IDENTIFICATION NUMBER
AFOSR/NA	NA	AFOSR-87-0143

8c. ADDRESS (City, State, and ZIP Code)	10. SOURCE OF FUNDING NUMBERS			
BUILDING 410 BOLLING AFB DC 20332-6448	PROGRAM ELEMENT NO.	PROJECT NO.	TASK NO.	WORK UNIT ACCESSION NO.
	61102F	2302	B3	

11. TITLE (Include Security Classification)

CRAZING IN POLYMERIC AND COMPOSITE SYSTEMS (u)

12. PERSONAL AUTHOR(S) HSIAO, C. C.

13a. TYPE OF REPORT	13b. TIME COVERED	14. DATE OF REPORT (Year, Month, Day)	15. PAGE COUNT
ANNUAL TECHNICAL	FROM 3/15/87 TO 3/14/88	1988, APRIL 30	

16. SUPPLEMENTARY NOTATION

17.	COSATI CODES		18. SUBJECT TERMS (Continue on reverse if necessary and identify by block number)
FIELD	GROUP	SUB-GROUP	polymeric, thermo-mechanical

19. ABSTRACT (Continue on reverse if necessary and identify by block number)

The study of the failure of composite systems under stress is important both theoretically and practically. This program aims to develop time dependent theories for studying crazing behavior of stressed polymeric and composite systems. Certain microstructural characteristics developed during deformation are considered in the mathematical formulations. This includes the development of basic analytical tools in creating possible constitutive modeling of thermo-mechanical behavior of polymeric and composite systems at combined micro- and macrostructural levels. This noncontinuum craze-crack transition is based on mesomechanical considerations which yield information upon damage micromechanics of crazing and failure behavior of polymeric and composite systems. (AW)

DTIC
ELECTE
AUG 2 5 1988

20. DISTRIBUTION / AVAILABILITY OF ABSTRACT	21. ABSTRACT SECURITY CLASSIFICATION
☒ UNCLASSIFIED/UNLIMITED ☐ SAME AS RPT. ☐ DTIC USERS	unclassified
22a. NAME OF RESPONSIBLE INDIVIDUAL George K. Haritos, Lt. Col., USAF	22b. TELEPHONE (Include Area Code) (202) 767-0463	22c. OFFICE SYMBOL NA

DD FORM 1473, 84 MAR   83 APR edition may be used until exhausted.   SECURITY CLASSIFICATION OF THIS PAGE
All other editions are obsolete.

88 8 25 152

UNCLASSIFIED

CRAZING IN POLYMERIC AND COMPOSITE SYSTEMS

TABLE OF CONTENTS AFOSR·TR· 88-0779

I.   INTRODUCTION

The study of an important and challenging problem in science and engineering has been the understanding of the strength and fracture behavior of stressed solid systems.   This is particularly true in the failure behavior and its prediction in viscoelastic material systems.   Both the structural and functional application of these materials demand a better understanding of their behavior and failure mechanisms. When sufficiently large tensile stresses are associated with these materials, various modes of failure develop.   To elucidate these, one common mode of response, namely crazing under an applied simple stress, must first be understood.   Major advances and breakthroughs in the crazing behavior in microscopic and macroscopic levels of understanding will yield tremendously useful information not only theoretically but also practically.   Considerable technological and scientific significance is attached to this proposed endeavor.   The initiation and propagation of crazing as quasifracture, the time dependent fracture strength of oriented polymers, the associated molecular orientation and ultimate strength in and around a craze, the interaction of crazes in polymeric and composite systems are just some of the features to be understood.   The determination of the time dependent fracture strength of polymers and composite systems, the displacement field and the stress distribution in the vicinity of craze-crack transition region as well as the propagation behavior of craze and crack are important problems to be solved prior to the consideration of many other relevant topics. Currently a firm foundation has been established.   It appears that continued research in the relevant outgrowth topics will result in a truly fruitful understanding of the subject matter.

II.   BACKGROUND INFORMATION AND OBJECTIVES, with REFERENCES

Advanced reinforced plastics, consisting of a polymer matrix and fibres, continue to generate great interest in their application to high performance structural components. Fracture of these composite systems may result from flaws in fibres or matrix as well as the failure of the bonds. Thus the strength of any such composite is governed by the time dependent strength characteristics of the matrix, the fibres and the bonds. Because of the difference in the mechanical behavior of the three constituents of composites, up to now many strength criteria have been considered and developed by scientists and engineers all over the world as reflected by, for example, several recent references [1 through 3].

The studies of time-dependent failure of composites have been relatively scarce in spite of the strong dependence of the failure characteristics on time. The formulation of the models must now be based upon the microstructural peculiarities of deformation, the molecular orientation, temperature and time. Aside from the phenomenological models, perhaps, statistical models should also be considered concurrently so that they may reinforce each other's findings and development.

REFERENCES

1.   *Handbook of Composites Series (Strong Fibres, Structure and Design, Failure Mechanics of Composites and Fabrication fo Composites).* Edited by A. Kelly and Yu. N. Rabotnove, North Holland (1985).

2.   *Proceedings of International Symposium on Composite Materials and Structures.* Edited by T. T. Loo and C. T. Sun, Beijing, China (June, 1985).

3.   M. F. Kanninen and C. H. Popelar. *Advanced Fractures Mechanics.* Oxford University Press, New York; Clarendon Press, Oxford (1985).

III.   MICROMECHANICS OF POLYMERS AND COMPOSITES

The phenomenon of crazing and its relation to some fracture analyses are considered as follows:

The formation of a craze comes about from a physical transformation in the deformation processes of the microscopic material molecules under tensile stress. The transformation takes place from a homogeneous deformation to a craze configuration when a critical condition is reached. Subsequently, the craze boundary propagates as a function of applied stress, time, temperature, physical and chemical influence as well as the actual microstructural changes subjected to geometrical constraints. As a result, usually minute voids are generated among oriented molecules and the density of the medium in the crazed region is nonuniformly reduced whereas the bulk of the homogeneous material body deforms more uniformly. The interface boundary layer enveloping crazes of many solid materials is capable of being drawn and transformed into bundles of highly oriented molecular domain structure in the craze region. Further stressing will eventually initiate craze-crack transition. It appears necessary to take these physical variations into consideration in any mathematical modeling and formulation in analyzing the stresses from the time when crazes incept to the time when they propagate and transform into real fractures.

The science of crazing, a quasifracture state, and subsequent cracking, a fracture state, of solid material systems under tension has been making large strides in the recent past. The crazing mechanism has been associated with molecular orientation and fracture strength [1 to 5]. Subsequently various methods have been utilized to determine and confirm the molecular mechanism with respect to craze formation and fracture in thermoplastics [5,6]. Essentially under tensile stresses certain solid materials deform from sites where high stress concentrations are created

and crazes develop. Because of geometrical constraints and energy requirements, the material molecules orient themselves in the direction of stressing with voids among them. As stated earlier, the presence of oriented polymeric molecules in a craze region bounded by surprisingly smooth interface layers is visualized as an actual physical phase transformation in the deformation processes from one orientation state to another depending upon the magnitude and rate of applied tensile stress [8], material characteristics as well as, of course, temperature and physical and chemical environments, etc., surround the solid body. As a result, the mechanical behavior of the material is greatly affected by the macroscopic geometry and the distribution and interaction of the individual crazes as well as the microscopic molecular configuration and voids within each craze region and along its immediate boundaries enveloping the area. Macroscopically the development of crazes and their distribution can be detected statistically by laser diffraction technique [9]. The geometry of an individual craze which can be studied by focused laser beams [10] is of primary importance in understanding the processes of its initiation and propagation as well as the deformation, quasifracture-fracture transition, and eventually the fracture behavior of the medium. Knowledge of craze initiation and geometry helps in determining the craze displacement field, the stress distribution and the craze-crack transition and propagation under load [11,12]. An eventual understanding of the true mechanism of molecular strength and fracture behavior of a simple solid matrix and a complex composite system can be obtained if fundamental microscopic information is utilized in macroscopic analyses.

In a craze the highly strained molecular bundles act as boundary tractions with great strength, any governing mathematical formulation must include this feature for any adequate analysis. Crazes of different forms and properties have occurred in

polymeric materials [13,14] and other solid systems including even single crystals [15]. An analysis is highly desirable and may be useful for studying general solid systems.

Both long- and short-range programs may be considered. It appears fruitful that emphasis be placed on the study of micromechanics of individual craze-crack transition, the source of failure under various internal and external stresses for the matrix and the composite systems.

The nature of the stresses in and around a craze-crack transition region is the key to the understanding of the morphology and nucleation as well as the propagation of crazes and cracks. The first attempt in calculating the state of macroscopic tensile stress field in the direction of the applied load as a function of craze length has been based upon a model with an assumed craze boundary displacement as a crack opening in an infinite elastic sheet [16]. The stresses were calculated as though the craze were a continuum and the craze boundary developed no stress perpendicular to the direction of applied stress. The solution of the two-dimensional-homogeneous biharmonic equation for a semi-infinite elastic medium due to the application of an external pressure to the surface has been used [17,18]. This implies that the craze behavior is independent of the craze medium [18,19] under stress. The solutions were obtained using a Fourier transform technique [20] or a complex variable method of analysis [19,21,22]. With proper assumed boundary conditions the latter method of approach gives probable stress and displacement fields surrounding a craze. A model for craze growth has also been considered with the creep of craze material as the cause of craze propagation. The craze growth was found to be linear with respect to the log of time [19].

The aforementioned stress analyses have been made essentially on the basis of the classical elasticity theory for a homogeneous elastic medium with either an

assumed stress distribution for certain portions of a crack without considering any time dependency.

The development of crazing is not only a function of stress but also a function of time [23,24]. Using the current theory and by taking into consideration the isotropic and anisotropic material constants the mathematical model describing the crazing mechanism have been successful [25].

REFERENCES

1.   J. A. Sauer, J. Marin and C. C. Hsiao, *J. Appl. Phys. 20*, 507 (1949).

2.   C. C. Hsiao and J. A. Sauer, *J. Appl. Phys. 21*, 1071 (1950).

3.   C. C. Hsiao, *J. Appl. Phys. 30*, 1492 (1959).

4.   C. C. Hsiao, Section IV in *Fracture Processes in Polymeric Solids*, Interscience, John Wiley, 529 (1964).

5.   S. R. Kao and C. C. Hsiao, *J. Appl. Phys. 35*, 3127 (1964).

6.   S. Rabinowitz and P. Beardmore, CRC Critical Reviews in *Macromolecular Science 1*, (1972).

7.   R. P. Kambour, *J. Poly Sci--Macromolucular Reviews 7*, 1 (1973).

8.   R. W. Truss and G. A. Chadwick, *J. Mat. Sci. 11*, 1385 (1976).

9.   C. C. Hsiao, *Appl. Phys.* Lett. *23*, 20 (1973).

10.   C. C. Hsiao, *J. Appl. Phys. 48*, 1168 (1977).

11.   A. P. Wilczynski, C. H. Liu and C. C. Hsiao, *J. Appl. Phys. 47*, 4301 (1976).

12.   A. P. Wilczynski, C. H. Liu and C. C. Hsiao, *J. Appl. Phys. 48*, 1149 (1977).

13.   H. H. Kausch and M. Dettenmaier, *Polymer Bulletin 3*, 565 (1980).

14.   M. Dettenmaier and H. H. Kausch, *Polymer Bulletin 3*, 571 (1980).

15.   K. F. Ha and Z. Z. An, *J. Appl. Phys. 55*, 95 (1984).

16. A. C. Knight, *J. Polymer Sci. 3A*, 1845 (1965).

17. H. C. Krenz, "Relationships Between Structure and Micromechanics of Solvent Crazes in Glassy Polymers," Ph.D. thesis, Cornell University, 115 (January, 1977).

18. N. Verheulpen-Heymans, *J. Polymer Sci. Phys. 14*, 93 (1976).

19. N. Verheulpen-Heymans and J. C. Bauwens, *J. Mat. Sci. 11*, 7 (1976).

20. B. D. Lauterwasser and E. J. Kramer, *Philo. Bull. 3*, 565 (1980).

21. N. I. Muskelishvili, *Some Basic Problems of the Mathematical Theory of Elasticity*, P. Noordhoff Groningen, 333 (1953).

22. T. Y. Fan, *Foundations of Fracture Mechanics* (in Chinese), Jiangsu Scientific and Technical Publisher, Jiangsu (December, 1978).

23. S. S. Chern and C. C. Hsiao, *J. Appl. Phys. 52*, (10) 5994 (1981).

24. S. S. Chern and C. C. Hsiao, *J. Appl. Phys. 53*, (10) 6541 (1982).

25. S. S. Chern, Z. D. Zhang and C. C. Hsiao, *J. Poly. Sci. Phys. 23*, 2579 (1985).

26. C. C. Hsiao and S. R. Moghe, *Characterization of Random Microstructural Systems*, Proceedings, International Conference on Structure, Solid Mechanics and Engineering Design in Civil Engineering Materials, Southampton, England, 1969, John Wiley, London, Part I, 95 (1971).

27. V. S. Kuksenko and V. P. Tamuzs, *Fracture Micromechanics of Polymer Materials*, Martinus Nijhoff Publishers, 202 (1981).

28. S. S. Chern and C. C. Hsiao, *J. Appl. Phys. 53*, 6541 (1982).

29. Z. D. Zhang, S. S. Chern and C. C. Hsiao, *J. Appl. Phys. 54*, 5568 (1983).

IV.   PROGRESS DURING THE FIRST YEAR   (See Appendix)

"Noncontinuum Craze-Crack Transition"

V. OUTLOOK FOR THE SECOND YEAR
(Work to be considered for publication)

1. "Crack-Induced-Craze"

The analysis of the crack-induced-craze in polymers is believed to be a fairly general phenomenon in fracture studies. This work will deal with the use of a viscoelastic boundary element method for analyzing a polymer quasi-fracture. A time dependent boundary stiffness will be considered and the viscoelastic solution in the time domain may be obtained by applying the collocation Laplace inversion technique. Using these methods, the quasifracture problem with time dependent stiffness fractions in a two-dimensional case may be analyzed. Both the craze opening displacement profile and the envelope stress distribution around a craze can be computed. This will pave the way in evaluating the propagation history of both the crack and the craze. Results thus obtained may be compared with those obtained by previous considerations such as the use of Dugdale model and the concern on the stress concentration phenomenon.

2. "Crazing as Quasifracture"

Before any real fracture develops under stress in polymeric or composite systems, it seems that a fairly general picture common to most solid systems, crazing incepts first. Following the previously stated craze-crack transition and crack-induced-craze, the initiation of crazing is simply a special case. In the absence of crack the craze as quasifracture has been studied by many scientists. Since the boundary element method has become recently a powerful technique for solving boundary value problems including some nonlinear ones, it is especially important as a tool to be used in problems

having viscoelastic deformations and fractures. Therefore, it may be fruitful in developing proper procedures for calculating the stress distributions around a craze envelope.

3. "Time Dependent Fracture Strength of Solid Bodies"

Statistical theories in fracture kinetics constitute a very important role in investigating the fracture strength of solids and their utilization in modern engineering. In this short report, a review of some of the recent concepts and models is provided. The main concern is the effect of the breaking stress on the time-to-break. Based upon the consideration of the fraction of integrity of a medium, a number of models have been evaluated and compared. Two basic considerations used for evaluation and comparison are Zhurkov's empirical kinetic relationship and Hsiao's statistical absolute reaction rate model. Other considerations reducible from these two are also given for comparison. Using a well-known numerical analysis method, it appears that the nonlinear mathematical consideration is more realistic in describing the time-dependent fracture strength behavior of a medium over any linear ones. The computed results seem to fit reasonably well with the general observations.

VI. OUTLOOK FOR THE THIRD YEAR
(Research to be conducted)

1. "Temperature Variation during Polymer Failure"

This paper attempts to discuss the temperature variation during polymer failure using a statistical absolute reaction rate theory. At fracture, the temperature may increase or decrease depending upon a quantity named fraction or integrity f and its rate $\dot{f}$ and accelerator $\ddot{f}$ as well as a stress modifier β.

For over a century, scientists and engineers have observed temperature variations during loading and testing of solids. Most work in this area focused on metallic systems: temperature changes during elastic and/or plastic deformations, as well as theoretical investigations based on mechanics and thermodynamics.

Using the statistical absolute reaction rate theory, the present work attempts to analyze the temperature variation during polymer failure.

2.   "Irradiation on Crazing Development"

The aerospace industry of the mid '80s is now being heavily involved in an unprecedented number of space projects which require the use of a diverse range of devices, all of which are exposed to much higher levels of radiation than the ones inside the earth's atmosphere. Polymeric materials are in common use although it is known that changes in their molecular structure are induced when exposed to high energy irradiation. The effects are not the same for all polymeric systems since some of them may degrade, others are induced to crosslinking and still others may crosslink to a saturation point and then degrade. In all cases, the mechanical properties are affected which implies changes on the performance and longevity of the material system.

At present there is a need to understand the mechanism responsible for these alterations as well as a model from which analysis and prediction of the polymer crazing behavior in environments exposed to radiation.

3.   "Three-Dimensional Crazing"

Polymers and polymeric composites usually fail by first developing crazing on the surface of the material system. Internal crazes can also be initiated when

sufficient and necessary conditions exist. The time-dependent craze failure process, whether two-dimensional or three-dimensional, may be characterized by several stages: deformation, development of microporosity, craze initiation, craze-crack transition and propagation until complete failure occurs. The interrelationship among the applied stress, craze initiation, time and temperature has been established and a fairly general time-dependent theory on craze initiation in viscoelastic media has been formulated. This craze initiation criterion is three-dimensional. It would be highly desirable to examine this new criterion and analyze the craze in three-dimensions.

VII. POSSIBLE FUTURE TOPICS AND THEIR IMPACT ON POLYMERIC AND COMPOSITE RESEARCH

"Analysis of Craze Interactions"
"Potential Energy Mimimization of Composite Matrix"
"Potential Energy of Fiber Reinforced Composite System"
"Elasticity Constants of Composites"
"Thermal Coefficients of Composites"

The aforementioned individual descriptions are some immediate projects to be completed and some others to be explored. Whenever possible time and temperature dependent stress analyses need to be introduced in the constitutive modeling of the mechanical behavior of composite systems at micro- and macro-structural levels. This interest is in the development of analytical methods as tools. To be followed are some experimental verifications and certain temperature data for quantitative analyses and numerical computations. It is hoped that these projects will have an impact leading to a better understanding of the effect of time and temperature on craze and fracture of composite systems.

VIII. SUMMARY

* Noncontinuum Craze-Crack transition yields damage behavior of composite systems.

* Studies of time dependent failure of composite systems are important practically and theoretically.

* Objectives are to obtain better understanding of the connection between microstructure and mechanics.

* An overall view is given during the first year, in the published paper "Non-Continuum Craze-Crack Transition."

* During the second year, several topical papers will be published. They are related to:

   "Crack-Induced-Craze"

   "Crazing as Quasifracture"

   "Time Dependent Fracture Strength of Solid Bodies"

* Some research work will be considered for the third year":

   "Irradiation on Crazing Development"

   "Three-Dimensional Crazing"

   "Temperature Variation During Polymer Failure"

* Possible future research topics:

   "Analysis of Craze Interactions"

   "Minimization of Potential Energy for Composite Matrix"

   "Minimization of Potential Energy for Composite Systems"

   "Analyses of Elasticity Constants of Composites"

   "Analyses of Thermal Coefficients of Composites"

* Six (6) copies of "Non-Continuum Craze-Crack Transition" are appended.

APPENDIX

NON-CONTINUUM CRAZE-CRACK TRANSITION

C. C. Hsiao
Department of Aerospace Engineering and Mechanics
University of Minnesota
Minneapolis, Minnesota

ABSTRACT

An approach studying the damage problem of polymeric and composite material systems is reviewed. It appears highly desirable to investigate the strength and fracture behavior of stressed solid systems by combining microstructural information with macro- mechanical analysis.

Starting from the initiation of crazes, the process of transition of a craze to crack in an infinite viscoelastic medium under stress is described. The actual physical change of a craze into a crack is considered. Emphasis is placed on the nature of its time dependency. The enlargement of both craze and crack is analyzed under a simple state of tension. Suggestions on future research upon temperature influence on crazing and craze-crack interactions are also given.

NOMENCLATURE

A,B	material constants
a_n	integer constants ($-\infty < n < \infty$)
$a(t)$	time-dependent length to high stress level σ_2
$b(t)$	time-dependent crack length measured from center of symmetry
$c(t)$	time-dependent craze-crack length measured from center of symmetry
$C_b(t)$	time-dependent material creep compliance function
$\dot{D}_f(t)$	rate of energy dissipation of craze fibril domains
$d(x,t)$	time- and position-dependent diameter of craze fibril domains
d_1	average diameter of fibril domain under craze envelope stress σ_1
d_2	average diameter of fibril domain under craze envelope stress σ_2
$E(t)$	relaxation modulus
e_{ij}	deviatoric strains
f	fraction of integrity of microstructural system
$G_1(t-\tau)$	time-dependent deviatoric relaxation modulus
$G_2(t-\tau)$	time-dependent dilatational relaxation modulus
$\dot{H}_c(t)$	rate of energy absorption of quadrantal craze
I_1, I_2	constants
$J_2(\xi-\eta)$	time dependent bulk creep compliance function
K_1, K_2, K_3, K_4	differential or integral functions
$K_b = \omega_b \exp[- U/RT + \beta \psi(t)]$	rate coefficient of breakage
$K_r = \omega_r \exp[- U/RT - \gamma \psi(t)]$	rate coefficient of reformation
$\dot{K}_f(t)$	rate of kinetic energy of craze fibril domains
n	integers
n_i, n_j	unit vectors (i, j = 1, 2 or 3)
$P(t)$	time-dependent load

dP	infinitesimal elemental vector in reference frame X_K ($K = 1, 2$ or 3)
dp	infinitesimal elemental vector in current frame x_k ($k = 1, 2$ or 3)
q	craze-crack system depth measured from center of symmetry
R	universal gas constant
S	magnitude of deviatoric stress tensor
$\mathbf{S}$	deviatoric stress tensor
s	Laplace parameter
S_{ij}	deviatoric stresses
$\dot{S}(t)$	rate of creation of craze fibril domain surface
T	absolute temperature
t	real time
t_a	time when $a(t)$ reaches position x
t_b	time-to-break
t_c	craze initiation time
t_f	craze-crack transition time
t_h	time when $b(t)$ reaches position x
t_n	nucleus incubation time
t_x	time for tip of craze-crack system to reach position x
t_2	period of time fibril domains subjected to stress σ_2
U	activation energy
$\dot{U}_f(t)$	rate of strain energy absorption of craze fibril domains
V_f	volume fraction of craze fibril domains
$u_{i,j}$	displacement gradients
$w(x,t)$	craze opening displacement measured from center of symmetry
$w_0(x,t) \equiv u_z(x,o,t),\ |x| < c(t)$.	opening displacement measured from center of symmetry of craze-crack system as defined
$x \equiv x_1$	coordinate along first coordinate axis
X_K	coordinates in reference frame ($K = 1, 2$ or 3)
x_k	coordinates in current frame ($k = 1, 2$ or 3)

$z \equiv x_3$	third coordinate axis
α_0	constant linear thermal coefficient of expansion
$\beta,\ \gamma$	positive parameters
δ_{ij}	delta function
$\Gamma_b,\ \Gamma_c$	material constants
ϵ	orientation strain $(-1 < \epsilon < \infty)$
ϵ_{kl}	strain tensor ($k, l = 1, 2$ or 3)
$\theta,\ \phi$	spherical coordinates
$\theta(T)$	temperature function
$\lambda(x,t)$	time- and position-dependent draw ratio
λ_1	draw ratio beyond craze mid-section under stress σ_1
λ_{m1}	draw ratio of craze mid-section at stress level σ_1
λ_{m2}	draw ratio of craze mid-section at stress level σ_2
ν	strain ratio
$\xi = t\phi(T),\ \eta = \tau\phi(T)$	shift times
n	strain ratio
ρ	density of the probability distribution function of molecular orientation
σ	applied stress
$\sigma_0(T,t)$	constant temperature, time-dependent stress
$\sigma_I,\ \sigma_{II}$	principal stresses
$\sigma_1,\ \sigma_2$	craze envelope stress levels
σ_b	tensile strength or fracture strength
σ_c	craze envelope stress
σ_{ij}	stress tensor ($i, j = 1, 2$ or 3)
$\dot{\sigma}_{ii}$	time derivative of the isotropic stress tensor
σ_{max}	maximum breaking stress
σ_{min}	minimum breaking stress
τ	time or dummy parameter
$\phi(x,t)$	stress function at spatial position x and time t

$\phi(T)$	temperature-time shift function
Ψ	axial stress of an element
$d\omega$	solid angle
ω_b	frequency of motion in breaking process
ω_r	frequency of motion in reforming process

PRELIMINARIES AND INTRODUCTION

For a long time, the analyses and prediction of the mechanical strength behavior of engineering components have been dependent mostly upon the application of continuum theories. This is true even in failure studies. Elasticity, viscoelasticity, plasticity and linear elastic fracture mechanics have dominated much of the analytical investigation in solid mechanics. Failure criteria for continuous media are considered to be independent with respect to the integrity of the media. There is no introduction of noncontinuum damage mechanics based upon microstructural behavior, and discrete interactions among discontinuous flaws are not predictable.

Recently, however, a new research direction has emerged to connect microscopic material behavior with macroscopic structural mechanics. This is motivated primarily by the strong desire to design the constitution and configuration of the microstructure of material systems for obtaining required macromechanical properties and functions. In doing so, the integrity of the media is included in failure criteria as well as in the constitutive description. Micromechanisms and their interactions are taken into consideration in analyses aside from their time and temperature dependencies.

In failure investigations of solids and composite material systems, an important and challenging problem in science and engineering has been the attempt to understand the strength and fracture behavior of stressed solid systems. Either continuum or noncontinuum method of approach has been used to study the problem. The continuum damage mechanics approach deals with the phenomenological behavior of matrix cracking in fiber-reinforced composites using quantities such as stress, strain, strain rate and temperature fields. The noncontinuum approach deals with the individual micro-damages such as minute crazes and cracks formed in the matrix together with the matrix-fiber interfaces in composites. Usual field quantities appropriate to the problem as well as unusual parameters are introduced to effect a satisfactory solution. During such a course of investigation, both micro- and macro-structural information is connected. This noncontinuum approach relies on the mode of damage and micromechanism. Aside from usual parameters, the ultimate results can depend upon other quantities such as a function of the fraction of integrity and/or a distribution function of molecular orientation, etc. The following gives an example concerning a noncontinuum micromechanics and craze-crack transition behavior.

Since the first publication of the pioneer work on crazing,[1] there was an inadvertent attempt to connect the microstructure of the polymer medium with its macroscopic behavior. However, little attention has been given to make this connection for many decades.

One of the first analyses of the growth of crazing was modeled as a continuum theory. Under a critical tensile stress the linearly elastic material initiates crazes which are rate insensitive.[2] Several other analyses using elasticity theory have also appeared more recently.[3,4] Similar to the analysis of a craze, many craze-related crack problems have been investigated in viscoelastic media.[5-10] The intention of these studies was to take care of the energy dissipation which takes place in the viscoelastic bodies not considered in the elastic theory. The time-dependent size and shape of cracks in linearly viscoelastic isotropic continuum media have been analyzed. No microstructural nature is considered however. Subsequently, approximate methods of analysis have been presented and illustrated with a failure zone to obtain viscoelastic stresses and displacements for elastic solutions. In the analysis, in order to satisfy the developed governing equations, the failure zone in the elastic problem is modified to meet the traction boundary condition for the crack faces. In general, the connection between the mechanics of the problem and the noncontinuum microstructural nature is not made in these investigations. Therefore, in the following example a noncontinuum craze-crack transition is analyzed in light of the actual microstructural behavior and the mechanics of the problem. Equations governing the rupture of the fibril domain structure in the middle of the craze envelope surfaces subject to a uniform tension is considered for an isolated craze in an infinite viscoelastic polymer sheet. Solutions yield both information on the time dependent craze-crack transition and the displacement field around the craze-crack envelope profile describing the shape of the craze-crack region. Before this is done relevant noncontinuum information is reviewed. Justifications and significance of using the noncontinuum microstructure are described.

TIME DEPENDENT DEFORMATION AND MOLECULAR ORIENTATION

By incorporating microstructural information, the deformation of a material system may be analyzed under stresses with the help of classical continuum theory. For some polymeric and composite systems, the deformation processes may be characterized to contain a molecular orientation mechanism with a microporosity sensitive to time and temperature.

A realistic medium may be represented by a system of microstructural elements which translate and rotate under stressing. As shown in Figure 1, an elemental vector dP in the reference frame X_K ($K = 1, 2, or 3$) transforms to dp in the current frame x_k ($k = 1, 2$ or 3) under a time-dependent load $P(t)$. Then the stress tensor σ_{ij} at any point can be calculated under certain conditions.[11]

$$\sigma_{ij}(\epsilon_{kl},T,t) = \int \rho(\theta,\phi,\epsilon_{kl}) \cdot f(\theta,\phi,\epsilon,T,t)$$

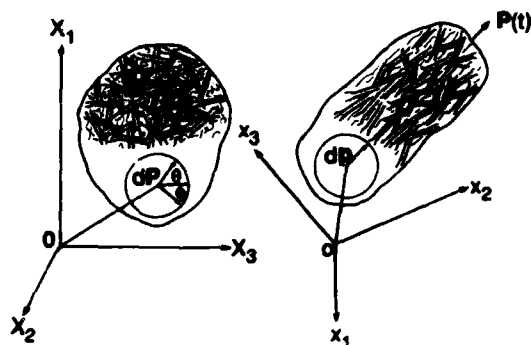$$\Psi(\theta,\phi,\epsilon,T,t) n_i n_j \, d\omega , \qquad (1)$$

Fig. 1 Molecular Entanglement and Orientation in Deformation

where ϵ_{kl} is the strain tensor,

T   is the absolute temperature,

t   is time,

ρ is the density of the probability distribution
        function of molecular orientation,

θ, ϕ are spherical coordinates,

f   is the fraction of integrity of the
        microstructional system,

ϵ is the orientation strain $(-1 < \epsilon < \infty)$,

Ψ is the axial stress in an element,

n_i, n_j are unit vectors, and

$d\omega$ equals $\sin\theta d\theta d\phi$ representing the solid angle
        from which statistical expectation may be
        evaluated.

Since the stresses are functions of the orientation
strain, it is likely that the constitutive behavior will be
greatly affected. A simple illustration is shown in Figure 2
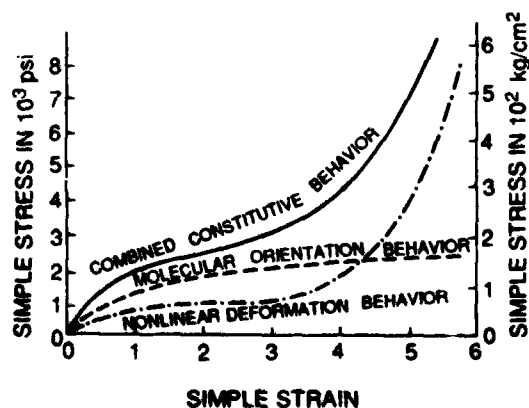
SIMPLE STRAIN

Fig. 2 Simple Stress-Strain Constitutive Behavior

where the nonlinear deformational behavior of an
isotropic continuum medium must be modified by the
molecular orientation behavior to give a more realistic
combined constitutive description. This no doubt will
affect the further response of the material system to
stressing such as the initiation of crazes and the stability
or instability of the system.

ENERGY STATE, TEMPERATURE AND CRAZE INITIATION

At a constant temperature, the stability of the
homogeneous deformation of a real material system
under a simple uniform tension will eventually be upset at
some time when a specific energy state of the
microstructural system develops. The possible responses
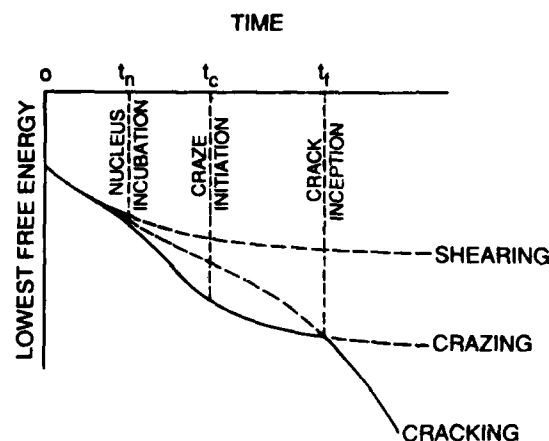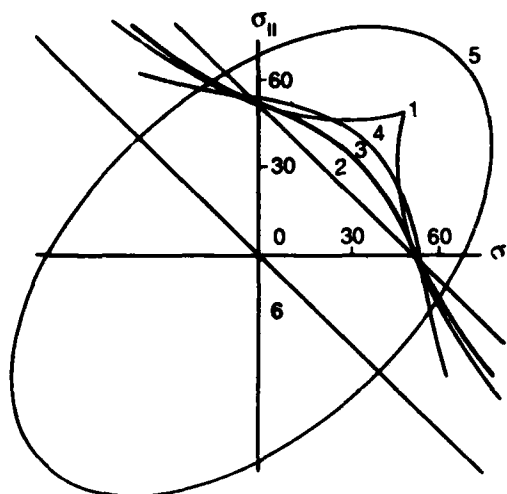may be described with the help of Figure 3. Under load,

Fig. 3 Lowest Free Energy State and Deformation Behavior

the stability or instability of a material system may best be
determined by its free energy state. The material system
readjusts its microstructural configuration to maintain its
lowest energy state until certain dominating
characteristics develop. After an incubation period is
reached the material system may deform in shear
primarily as a result of the rotational motion of certain
microstructures. Thus, a simple shearing band develops
in the system. The material system may develop cracks
as a result of a basically translational motion of the
microstructure including possibly the slipping and
rupturing of molecular bonds. This may be the simple
cracking of a material system. When a complex kinetic
situation occurs, both the rotational and translational
motion of the microstructure may take place. Crazing may
develop as a result.

For a two-dimensional craze, the isochronous
biaxial locus for craze initiation is given in Figure 4.
Various criteria put forward to date are plotted for
comparison. Detailed information can be found in an
earlier reference.[12] Only the three-dimensional craze
initiation criterion is given below in a series form with a_n
as an integer constant and n an integer.

Fig. 5 Stress, Temperature Effects on
Craze Initiation in Polymers

Stress in MPa

Biaxial locus for criteria of craze initiation in polymers by:
1. Sternstein and Ongchin,
2. Bowden and Oxborough,
3. New Criterion,
4. Argon,
5. Distortion strain energy, and
6. 45° reference line

Fig. 4 Biaxial Locus for Criteria of Craze Initiation in Polymers

$$S(x_k, T, t) \geq \sum_{n=-\infty}^{\infty} a_n [3\alpha_o \Theta(T)$$

$$+ \int_{-\infty}^{t} J_2(\xi - \eta)\dot{\sigma}_{ii}(x_k, \tau) \, d\tau]^n \qquad (2)$$

where S is the magnitude of the deviatoric stress tensor S which must overcome an intrinsic flow resistance, a_n are constants, α_o is the constant linear thermal coefficient of expansion, $\Theta(T)$ is the temperature function, $J_2(\xi - \eta)$ is the bulk creep compliance function with $\xi = t\phi(T)$ and $\eta = \tau\phi(T)$ as shift times defined by the "temperature-time shift" principle for "thermorheologically simple" viscoelastic media and $\dot{\sigma}_{ii}$ is the time derivative of the isotropic stress tensor. This three-dimensional craze initiation criterion is reducible to any of the other criteria by introducing appropriate values for a_n. In Figure 4 this new criterion is represented by line 3 for the two-dimensional situation. This line reduces to each of the other curves from 1 through 5 when appropriate values of a_n and n are introduced.

The influence of temperature motion on craze-initiation is also plotted in Figure 5 together with the applied stress for the polystyrene material system computed with $a_0 = -30$ MN/m^2, $a_{-1} = 0.3$ MN/m^2 and $a_1 = 0$.

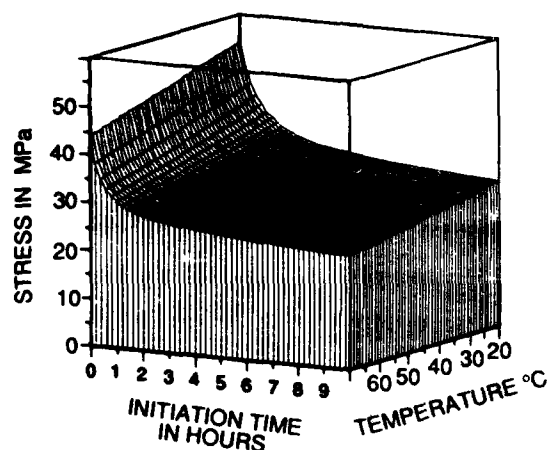## MICROSTRUCTURE AND MECHANICAL STRENGTH

Based upon the microstructural behavior and the dynamic nature of molecular motion, the fraction of integrity can be determined and utilized to establish a fracture criterion for a material system. Subsequently the connection between the microstructure and the macromechanical strength can be made. This has been done by means of the statistical theory of the absolute reaction rate. Not only can the microstructural orientation and the rupture of the microscopic structural units be incorporated but their reformation can also be included in the theory to obtain the time-dependent mechanical strength particularly for long times as illustrated in Figure 6.[11,13-15] This tensile strength which is the fracture strength as a function of time has been well established as shown. The tensile strength of a stressed solid material system for both short or long times tends to level off as shown. This means that the tensile strength becomes independent of time for very short times as well
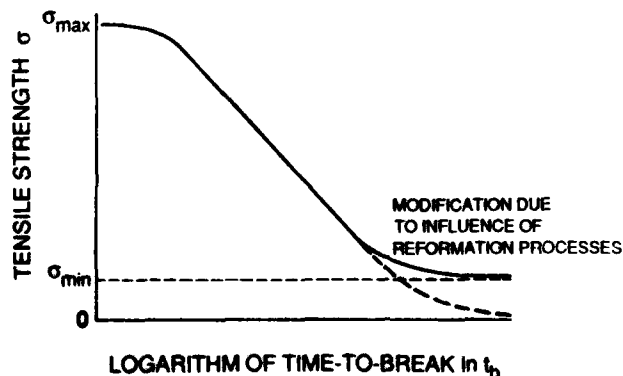

Fig. 6 Microstructural Orientation and Reformation Effects on a
Time-Dependent Mechanical Strength

as for very long times. In between these times, the tensile strength is linearly proportional to the logarithm of time. The temperature effect on the time-dependent mechanical strength is given in Figure 7 to show that temperature is an important entity in this complex situation which must be taken into consideration in the analysis for any material system.
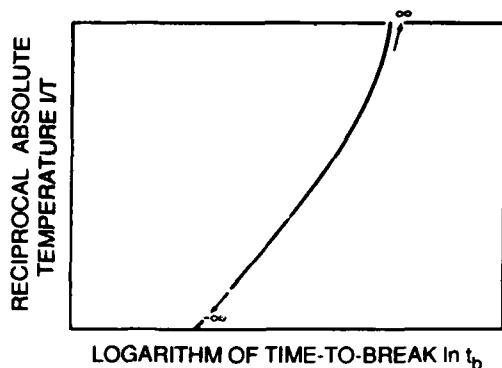

Fig. 7 Temperature Effects on Time-Dependent
Mechanical Strength

Consider a material system composed of a large number of randomly oriented similar molecular units or elements which elongate and rotate in a stress field. In order to formulate a temperature- and time-dependent failure criterion for such a material system, one can use the quantity $f(t)$, the time-dependent fraction of integrity. By calculating its time rate of change as follows:

$$\dot{f} = K_r(1-f) - K_b f \qquad (3)$$

where $K_r = \omega_r \exp[- U/RT - \gamma \Psi(t)]$ is the rate coefficient of reformation of the disconnected units and $K_b = \omega_b \exp[- U/RT + \beta \Psi(t)]$, the rate coefficient of breakage of the connected elements, ω_r and ω_b are respectively the frequencies of motion with respect to forming and breaking processes of these units, U is the activation energy, R is the universal gas constant, and γ and β are positive parameters which modify the true axial stress $\Psi(t)$ in each elemental unit.

The failing of a material system is when f approaches zero. In these formulations, K_r and K_b, are both functions of temperature and the true stress in individual elements. Once a stress σ is applied to the material system, the energy state is altered and the time-to-break t_b can be calculated.

The fracture strength, the statistical mean strength in the vicinity of any point in the system, has been analyzed and found to be proportional to the modulus of individual elements, their length and the number of the elements per unit volume. For an oriented system, the fracture strength is a function of deformation as briefly reviewed in the previous section. For a fully oriented system[11] under a constant applied stress σ, we may write

$$\Psi(t)f(t) = \sigma . \qquad (4)$$

The functional relationship between Ψ and t is

$$\Psi = - \frac{\Psi^2}{\sigma}[K_r(1 - \frac{\sigma}{\Psi}) - K_b \frac{\sigma}{\Psi}] . \qquad (5)$$

Integration results in the time-to-break t_b. With zero initial time

$$t_b = \int \frac{d\Psi}{\Psi[K_b + K_r(1 - \Psi/\sigma)]} . \qquad (6)$$

Usually near fracture, K_r becomes unimportant, and the time-to-break may be approximated to

$$t_b = \exp(U/RT) \int \frac{d\Psi}{\omega_b \Psi \exp(\beta \Psi)} , \qquad (7)$$

which can further be simplified to

$$t_b = A\exp(- B\sigma) \qquad (8)$$

with A and B as material constants.

Now let us consider the craze problem as shown in Figure 8. Under a temperature and time dependent stress $\sigma_0(T,t)$ a three-dimensional craze may develop from the surface of a material body. In general the microstructure on the surface of the material body is composed of a network of highly oriented fibril domains drawn out of the envelope profile and separated by cavities. This combined structure propagates along the surface of the material body and penetrates into the body as indicated respectively by $c(T,t)$ and $q(T,t)$ which are measured from the center of craze at the origin 0. The stress at any point in the material is designated as $\sigma(x_1,x_2,x_3,T,t)$ and the craze envelope stress by $\sigma_c(x_1,x_2,x_3,T,t)$ as shown.
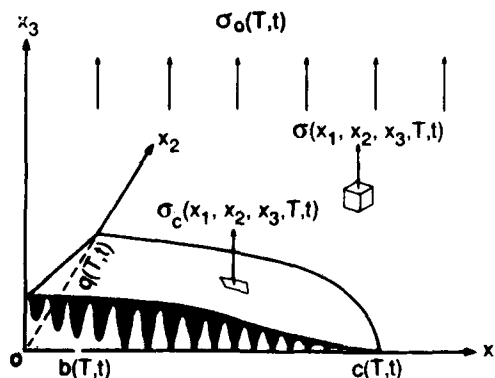

Fig. 8 Microstructure of a Three-Dimensional
Craze-Crack System

A strong interest has been the determination of the displacement field since it is not easily measured. This noncontinuum feature is easily seen in Figure 9, in which the randomly oriented microstructure is being drawn into
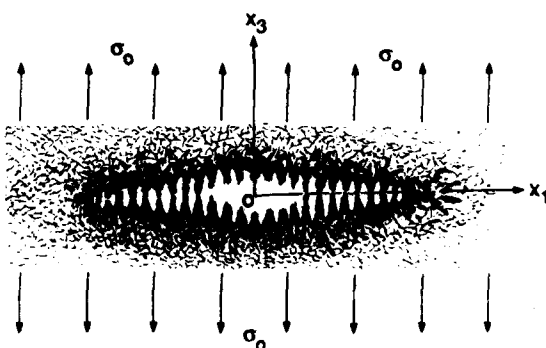
Fig. 9 Microstructural Formation of a Two-Dimensional
Craze-Crack System

highly oriented fibril domains. A schematic diagram of a two-dimensional craze is given in Figure 10 to show the pertinent quantities. For simplicity in sequel x_3 is replaced by z and x_1, by x.
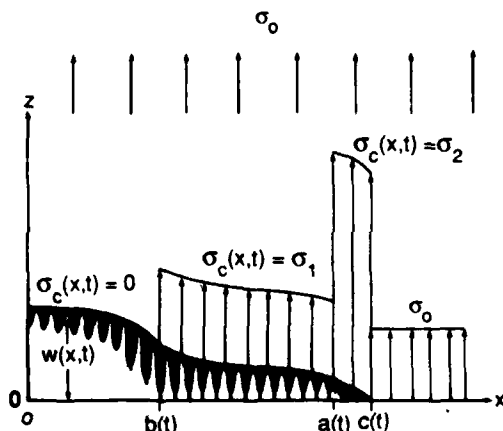

Fig. 10 An idealized Two-Dimensional Craze-Crack System
with Assumed Step Envelope Stress Distribution

ANALYSIS OF CRAZE-CRACK TRANSITION

Considering this two-dimensional model, an analysis can be made to obtain the time dependent displacement field and the craze-crack lengths by incorporating the microstructural behavior into the macromechanics problem.

Starting from the highly oriented fibril domain structure in the craze region, the required time-to-break t_b is calculable based upon a perfectly oriented molecular system under a constant stress σ.[11],[15] A general curve t_b vs. σ is given in Figure 6. The maximum applied stress is indicated by σ_{max}. With reformation processes considered, the tensile strength of the material system begins to deviate from the dotted curve. There exists a minimum strength value σ_{min} for which t_b goes to infinity asymptotically.[14] Therefore for a given medium there

exists a corresponding curve between t_b and the applied constant stress σ. When the applied stress varies with time, one can use the linear summation damage rule which states that the same number of damages accumulate during identical time intervals. Thus the time-to-break is determinable by the equation:[16]

$$\int_0^{t_b} \frac{dt}{t_b[\sigma(t)]} = 1. \tag{9}$$

By adopting this microstructural behavior, the opening displacement $w(x,t)$, the craze-crack system length $c(t)$ and the crack length $b(t)$ in this craze-crack transition problem can be calculated. To facilitate the possibility of obtaining numerical solutions, a three-step envelope stress distribution, as shown in Figure 10, is introduced:

$$\sigma_c(x, t) = \begin{bmatrix} 0 & o < x < b(t), \\ \sigma_1 & b(t) < x < a(t), \\ \sigma_2 & a(t) < x < c(t). \end{bmatrix} \tag{10}$$

It is hoped that this assumed step stress function will yield good approximations in both the displacement field and the lengths of the craze-crack system.[1]

With the three-step envelope stress function, the stress sustained by the fibril domains in the thin mid-section where under certain conditions, failure has been observed to occur more often, is

$$\begin{bmatrix} \sigma = \lambda_{m2}\sigma_2 & a(t) < x < c(t), \\ \sigma = \lambda_{m1}\sigma_1 & b(t) < x < a(t), \end{bmatrix} \tag{11}$$

where $\lambda_{m2}\sigma_2$ is the true stress born by the fibril domains and λ_{m2} is the draw ratio at the stress region σ_2. Similarly $\lambda_{m1}\sigma_1$ and λ_{m1} denote the corresponding quantities under region σ_1.

As discussed earlier, under large stresses, the time-to-break t_b can be obtained by first dropping K_r in (3) to get (8), then introducing (11) in (9), one can obtain:

$$t_b = A\exp(-B\lambda_{m1}\sigma_1)$$

$$- t_2\{\exp[B(\lambda_{m2}\sigma_2 - \lambda_{m1}\sigma_1)] - 1\} \tag{12}$$

where t_2 is the period when the fibril domains experience the higher envelope stress σ_2.

To review briefly the time-dependent viscoelastic problem, the opening displacement measured from the center of symmetry of the craze-crack system in a viscoelastic polymer sheet can be obtained by using the well known correspondence principle in linear viscoelasticity.

The field equations are:

$$\sigma_{ij}(x,z,t) = 0, \tag{13}$$

31

$$\epsilon_{ij}(x,z,t) = \frac{1}{2}[u_{i,j}(x,z,t) + u_{j,i}(x,z,t)] \, , \tag{14}$$

$$S_{ij}(t) = \int_{-\infty}^{t} G_1(t-\tau)de_{ij}(\tau) \, , \tag{15}$$

$$\sigma_{ij}(t) = \int_{-\infty}^{t} G_2(t-\tau)d\epsilon_{ij}(\tau) \, , \tag{16}$$

where σ_{ij} is the stress tensor, ϵ_{ij}, the strain tensor, $u_{i,j}$, the displacement gradients, G_1 and G_2 are respectively the deviatoric and dilatational relaxation moduli of the original bulk medium, and the deviatoric stresses and strains are respectively

$$S_{ij}(t) = \sigma_{ij}(t) - \frac{1}{3}\delta_{ij}\sigma_{kk}(t) \, , \tag{17}$$

$$e_{ij}(t) = \epsilon_{ij}(t) - \frac{1}{3}\delta_{ij}\epsilon_{kk}(t) \, , \tag{18}$$

with i, j and k = x or z denoting dummy variables in two-dimensional problems. The boundary conditions are described as:

$$\sigma_{zx}(x,o,t) = 0 \, , \qquad |x| < c(t) \tag{19}$$

$$\sigma_{zz}(x,o,t) = \sigma_c(x,t) \, , \quad |x| < c(t) \tag{20}$$

$$\left.\begin{array}{l} \sigma_{zz}(x,z,t) = \sigma_0(t) \, , \\[2mm] \sigma_{xx}(x,z,t) = 0 \, , \\[2mm] \sigma_{xz}(x,z,t) = 0 \, , \end{array}\right\} \quad \text{as } (x^2+z^2) \to \infty \, . \tag{21}$$

The opening displacement $w_0(x,t)$ is defined by

$$w_0(x,t) = u_z(x,o,t) \, , \qquad |x| < c(t) \, . \tag{22}$$

To solve this viscoelastic problem. The Laplace transform with respect to time is applied to all of the field equations and the boundary conditions. The solution to the transformed equation can be found by using the well established complex variable conformal mapping method or the complex variable stress function method for elastic medium.

The time dependent solution of the problem is obtained by Laplace inversion. This solution is valid only if the boundary conditions are independent of time, i.e., $\wedge(t)$, b(t) and $\sigma_c(x,t)$ remain unchanged. These restrictions can be removed by using a sequence of loading and unloading steps,[17] which yields,

$$w_0(x,t) = C_b(o)\Phi(x,t) + \int_{0}^{t} \dot{C}_b(t-\tau)\Phi(x,\tau)d\tau \, , \tag{23}$$

where

$$\Phi(x,t) = \sigma_0\sqrt{c^2-x^2} - \frac{2}{\pi}\int_{0}^{c} \sigma_c(\xi,t) \ln(c+\sqrt{c^2-\xi^2})d\xi$$

$$+\frac{2}{\pi}\int_{0}^{x} \sigma_c(\xi,t) \ln(x + \sqrt{x^2-\xi^2})d\xi$$

$$+\frac{2}{\pi}\int_{x}^{c} \sigma_c(\xi,t) \ln\xi d\xi \, , \tag{24}$$

$$C_b(t) = L^{-1} [(2(2\overline{G}_1+\overline{G}_2)) / (s^2\overline{G}_1(\overline{G}_1+2\overline{G}_2))] \tag{25}$$

with L^{-1} designating the Laplace inversion and barred quantities being in Laplace domains.

If the strain ratio ν is constant, $C_b(t)$ reduces to

$$C_b(t) = L^{-1} [(2(1 - s^2\nu^2)) / s^2\overline{E}] \, , \tag{26}$$

where E is the relaxation modulus of the original unoriented bulk polymer medium.

Taking into consideration the thickness of the primordial layer from which the fibril domain structure has been pulled out, the actual opening displacement of the system becomes

$$w(x,t) = C_b(o)\Phi(x,t) + \int_{0}^{t} \dot{C}_b(t-\tau)\Phi(x,\tau)d\tau$$

$$+\int_{t_x}^{t} \frac{\dot{w}(x,\tau)}{\lambda(x,\tau)}d\tau \, , \tag{27}$$

where t_x is the time when the tip of the craze-crack system first reaches the point x, λ is the draw ratio. Since the midsection is relatively thin in a craze, the λ function can be taken as

$$\lambda(x,t) = \left[\begin{array}{ll} \lambda_1 \, , & b(t) < x < a(t) \\[4mm] \lambda_{m2} \, , & a(t) < x < c(t) \, , \end{array}\right. \tag{28}$$

where λ_1 is the draw ratio outside the mid-section under the envelope stress σ_1. The opening displacement finally is obtained as

$$w(x,t) = \frac{\lambda_{m2}}{\lambda_{m2}-1}[C_b(o)\Phi(x,t)$$

$$+ \int_{0}^{t} \dot{C}_b(t-\tau)\Phi(x,\tau)d\tau] \, , \quad \text{for } a(t) < x < c(t), \tag{29}$$

$$w(x,t) = \frac{\lambda_1}{\lambda_1-1}[C_b(o)\Phi(x,t) + \int_{0}^{t} \dot{C}_b(t-\tau)\Phi(x,\tau)d\tau]$$

$$+ (\frac{1}{\lambda_{m2}} - \frac{1}{\lambda_1})w(x,t_a) \, , \qquad \text{for } b(t) < x < a(t), \tag{30}$$

$$w(x,t) = C_b(o)\Phi(x,t) + \int_{0}^{t} \dot{C}_b(t-\tau)\Phi(x,\tau)d\tau$$

32

$$+ \left(\frac{1}{\lambda_{m2}} - \frac{1}{\lambda_1}\right) w(x,t_a) + \frac{1}{\lambda_1} w(x, t_h) ,$$

$$\text{for } o < x < b(t) , \qquad (31)$$

where t_a and t_h respectively denote the times when $a(t)$ and $b(t)$ arrive at the point x.

CRAZE AND CRACK LENGTHS

With regard to the length of the craze-crack system and that of the crack, suppose that the fibril domain nucleation rate at the craze tips is proportional to the growth velocity $\dot{c}(t)$ of the system. Then the energy rate required for the growth of craze tip is $\Gamma_c \dot{c}(t)$ and that for the crack tip is $\Gamma_b \dot{b}(t)$, where Γ_c and Γ_b are material constants. Based upon the assumption that the rate of energy required for drawing the fibrils out of the craze surface envelope is proportional to the rate of creation of the new fibril domain surface $\dot{S}(t)$, using the proportionality constant Γ_s, the following local energy balance equation can be written as:

$$\dot{H}_c(t) = \Gamma_c \dot{c}(t) + \Gamma_b \dot{b}(t) + \Gamma_s \dot{S}(t)$$

$$+ \dot{U}_f(t) + \dot{D}_f(t) + \dot{K}_f(t) \qquad (32)$$

where $\dot{H}_c(t)$ is the energy absorption rate of the quadrantal portion of the craze system, $\dot{U}_f(t)$ is the strain energy absorption rate of fibril domains, $\dot{D}_f(t)$ is the energy dissipation rate by the craze fibrils, and $\dot{K}_f(t)$ is the rate of kinetic energy due to the motion of the craze fibril domains. $\dot{U}_f$, $\dot{D}_f$ and $\dot{K}_f$ are negligible when compared with the other rate quantities in the quasi-static conditions. With this simplification and the terms expressed by elementary parameters defined earlier, the following equations can be established. Since the stress each fibril domain sustains is $\lambda \sigma_c$ which equals σ_c/V_f if V_f is the volume fraction:

$$\dot{H}_c(t) = \int_0^c \sigma_c(x,t) \frac{\partial w(x,t)}{\partial t} dx , \qquad (33)$$

$$\dot{S}(t) = \int_0^c 4 \frac{V_f(x,t)}{d(x,t)} \frac{\partial w(x,t)}{\partial t} dx , \qquad (34)$$

where $d(x,t)$ is the time and position dependent diameter of craze fibril domains. Now using these, Equation (32) becomes an implicit nonlinear differential equation of the craze-crack system length $c(t)$ and the crack length $b(t)$ as follows:

$$\int_0^c \left(\sigma_c - 4 \frac{\Gamma_s V_f}{d}\right) \frac{\partial w(x,t)}{\partial t} dx = \Gamma_c \dot{c} + \Gamma_b \dot{b} . \qquad (35)$$

This implicit differential equation has three unknown quantities, $a(t)$, $b(t)$ and $c(t)$ to be determined. In order to solve this equation, some subsidiary equations are necessary. One of them is that[17] the craze envelope stress $\sigma_c(x,t)$ must balance the applied external load corresponding to an applied simple tension σ_0 to ensure that the stress field within the uncrazed bulk material is finite everywhere for all times t. In mathematical form this means:

$$\int_0^c \frac{\sigma_c(x,t)}{\sqrt{c^2(t)-x^2}} dx = \frac{\pi}{2} \sigma_0 . \qquad (36)$$

When the three-step envelope stress function (10) is substituted in, it yields:

$$a(t) = c(t) \sin\left(\frac{\pi}{2} \frac{\sigma_2-\sigma_0}{\sigma_2-\sigma_1} - \frac{\sigma_1}{\sigma_2-\sigma_1} \sin^{-1} \frac{b(t)}{c(t)}\right) . \qquad (37)$$

The other equation is from the consideration of the nature of the failure of the craze material, which obviously provides a relation between the craze-crack system and crack lengths,

$$b(t) = c(t - t_b) . \qquad (38)$$

It should be noted that the time-to-break t_b is spatially dependent and it is evident that

$$b(t) = c[t - t_b(b(t))] . \qquad (39)$$

RESULTS AND DISCUSSION

Generally speaking, $c(t)$ and $b(t)$ can be obtained as functions of time by solving Equations (35), (37) and (39). But it is still rather complicated because of the unusual form of Equation (39).

If the craze-crack system and the crack propagate steadily without drastically change in their propagating speeds, Equation (39) can be simplified to the following form

$$b(t) = c(t) - t_b \dot{c}(t) , \qquad (40)$$

where t_b has been evaluated and displayed as Equation (12), i.e.,

$$t_b = A \exp(-B\lambda_{m1}\sigma_1)$$

$$- t_2 \{ \exp[B(\lambda_{m2}\sigma_2 - \lambda_{m1}\sigma_1)] - 1 \} .$$

Usually, the distance $c(t) - a(t)$ is relatively small since it is associated with the region of stress concentration. Thus t_2 can be expressed as

$$t_2 = (c - a) / \dot{c} . \qquad (41)$$

Using the envelope stress profile proposed earlier, Equation (24) turns out to be

$$\Phi = \frac{1}{\pi} [(\sigma_2-\sigma_1)x \ln \frac{a\sqrt{c^2-x^2} - x\sqrt{c^2-a^2}}{a\sqrt{c^2-x^2} + x\sqrt{c^2-a^2}}$$

$$+ \sigma_1 x \ln \frac{b\sqrt{c^2-x^2} - x\sqrt{c^2-b^2}}{b\sqrt{c^2-x^2} + x\sqrt{c^2-b^2}}$$

$$- (\sigma_2 - \sigma_1) a \ln \frac{\sqrt{c^2 - x^2} - \sqrt{c^2 - a^2}}{\sqrt{c^2 - x^2} + \sqrt{c^2 - a^2}}$$

$$- \sigma_1 b \ln \frac{\sqrt{c^2 - x^2} - \sqrt{c^2 - b^2}}{\sqrt{c^2 - x^2} + \sqrt{c^2 - b^2}}] . \tag{42}$$

Since the product of the average fibril domain diameter and the envelope stress has been found to be constant, that is, $d_1 \sigma_1 = d_2 \sigma_2 = $ constant, thus let

$$d(x, t) = \begin{bmatrix} d_1, & b(t) < x < a(t), \\ d_2, & a(t) < x < c(t), \end{bmatrix} \tag{43}$$

and noting that $V_f = 1/\lambda$ and Equation (32) then, by substitution, Equation (35) becomes

$$(\sigma_2 - \frac{4\Gamma_s}{d_2 \lambda_{m2}}) \int_a^c \frac{\partial w}{\partial t} dx$$

$$+ (\sigma_1 - \frac{4\Gamma_s}{d_1 \lambda_1}) \int_b^a \frac{\partial w}{\partial t} dx = \Gamma_c \dot{c} + \Gamma_b \dot{b} . \tag{44}$$

Since $\Phi(c, t) = o$, obviously,

$$\int_a^c \frac{\partial w}{\partial t} dx = \frac{\lambda_{m2}}{\lambda_{m2} - 1} \{ C_b(o)[\dot{a}\Phi(a,t)$$

$$+ \frac{d}{dt} \int_a^c \Phi(x,t)dx]$$

$$+ \int_a^c \dot{C}_b(o)\Phi(x,t)dx$$

$$+ \int_a^c \int_o^t \dot{C}_b(t-\tau)\Phi(x,\tau)d\tau dx \} , \tag{45}$$

$$\int_b^a \frac{\partial w}{\partial t} dx = \frac{\lambda_1}{\lambda_1 - 1} \{ C_b(o) [\dot{b}\Phi(b,t) - \dot{a}\Phi(a,t)$$

$$+ \frac{d}{dt} \int_b^a \Phi(x,t)dx]$$

$$+ \int_b^a \dot{C}_b(0)\Phi(x,t)dx$$

$$+ \int_b^a \int_o^t \ddot{C}_b(t-\tau)\Phi(x,\tau)d\tau dx \} . \tag{46}$$

Introducing the notations

$$\Phi_{ac} = \int_a^c \Phi(x,t)dx , \tag{47}$$

$$\Phi_{ba} = \int_b^a \Phi(x,t)dx , \tag{48}$$

and substituting them into (44), we have

$$K_1 \dot{a}(t) + K_2 \dot{b}(t) + K_3 \dot{c}(t) + K_4 = o , \tag{49}$$

where

$$K_1 = C_b(o)[(I_2 - I_1)\Phi(a,t) + I_2 \frac{\partial \Phi_{ac}}{\partial a} + I_1 \frac{\partial \Phi_{ba}}{\partial a}] , \tag{50}$$

$$K_2 = C_b(o)\{ I_2 \frac{\partial \Phi_{ac}}{\partial b} + I_1 \{ \Phi(b,t) + \frac{\partial \Phi_{ba}}{\partial b} \} \} - \Gamma_b , \tag{51}$$

$$K_3 = C_b(o)(I_2 \frac{\partial \Phi_{ac}}{\partial c} + I_1 \frac{\partial \Phi_{ba}}{\partial c}) - \Gamma_c , \tag{52}$$

and

$$K_4 = \dot{C}_b(o)(I_2 \Phi_{ac} + I_1 \Phi_{ba})$$

$$+ I_2 \int_o^t \ddot{C}_b(t-\tau)\Phi_{ac}d\tau + I_1 \int_o^t \ddot{C}_b(t-\tau)\Phi_{ba}d\tau , \tag{53}$$

with I_1 and I_2 being constants, and

$$I_1 = (\sigma_1 - \frac{4\Gamma_s}{d_1 \lambda_1}) \frac{\lambda_1}{\lambda_1 - 1} , \tag{54}$$

$$I_2 = (\sigma_2 - \frac{4\Gamma_s}{d_2 \lambda_{m2}}) \frac{\lambda_{m2}}{\lambda_{m2} - 1} . \tag{55}$$

The explicit forms of those quantities in expressions of K's are given in the Appendix.

The calculations should be divided into two steps. First, the original craze propagates during the absence of a crack. This can be calculated by simply setting $b(t) = o$ in Equations (38) and (44), which degenerates into the case discussed earlier.[17] After certain time elapses, the fibril domains first produced in the mid-section of the craze breaks down and crack commences. Second, the crack comes into play and the Equations (38), (41), (42) and (44) must be used to calculate simultaneously the propagations for both the craze-crack system and the crack.

Now to illustrate the changes of a craze-crack system in polystyrene, a Voigt solid is taken as an example. The material properties are taken to be[18-23]

$$J(t) = \{29 + 5.09[1 - \exp(-t)] + 2.32[1 - \exp(-t/10)]$$

$$+ 6.59[1 - \exp(-t/10^2)] + 12.72[1 - \exp(-t/10^4)]$$

$$+ 0.71[1 - \exp(-t/10^5)] + 14.71[1 - \exp(-t/10^6)]$$

$$+ 1.02[1 - \exp(-t/10^7)]\} \cdot 10^{-5} \; m^2/MN,$$

$A = \exp(11)$ secs, $\qquad d_1 = 20$ nm,

$B = 0.05 \; m^2/MN,$ $\qquad d_2 = 10$ nm,

$\lambda_1 = 2.0,$ $\qquad \Gamma_s = 0.125 \; J/m^2,$

$\lambda_{m1} = 2.5,$ $\qquad \Gamma_c = 0.085 \; J/m^2,$

$\lambda_{m2} = 4,$ $\qquad \Gamma_b = 300 \; J/m^2.$

ν for polystyrene is 0.395, a constant, and the applied stress is considered to be 36 MN / m^2, that is: $\sigma_0 = 36$ MN / m^2. In addition, based upon some experimental evidence, σ_1 and σ_2 are assumed to be respectively 40 MN / m^2 and 80 MN / m^2 for numerical calculations.

The normalized length of the craze-crack system and that of the crack are shown in Figure 11, where the
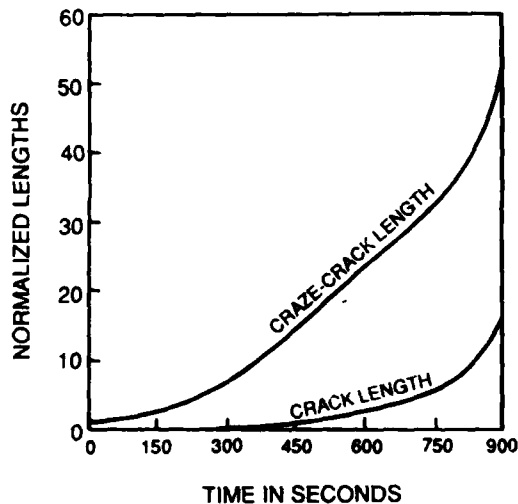

Fig. 11 Time-Dependent Crack and Craze-Crack
System Lengths

normalization is made with respect to the initial length of the craze-crack system. The opening displacements at different times are plotted in Figure 12.

For ease of visualization, the normalized craze length as a function of time is also given in Figure 13. The non-linear nature of the craze behavior is self-evident.

As can be seen from the calculations, both the velocities of the craze-crack system and that of the crack become larger and larger. Thus further calculation is not accurate since the unsteady propagation gives rise to irregular growth, branching and/or bifurcation. These

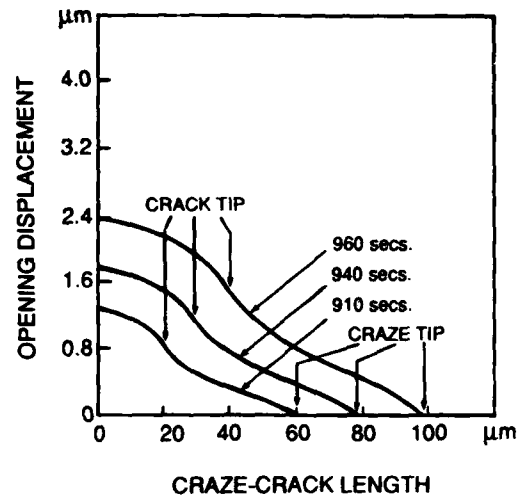complex phenomena are yet to be considered in the future analyses.

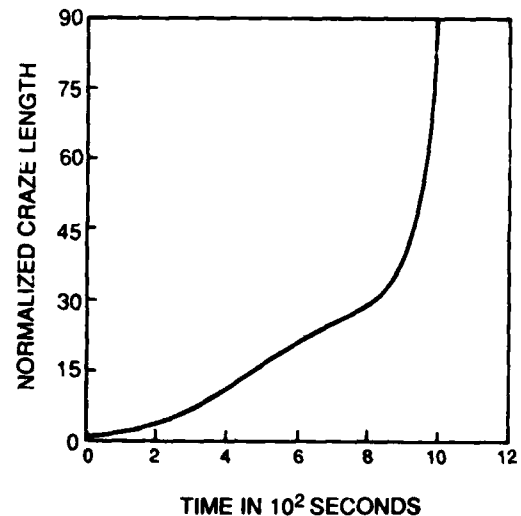Fig. 12 Nonlinear Crack and Craze-Crack Length Behavior

Fig. 13 Nonlinear Behavior of Normalized Craze Length

REMARKS AND SUGGESTIONS

From the review of the connection between microstructure and macromechanics as well as the analysis of the craze-crack transition it is seen that, in general, the complete fracture processes take time to develop and mature. Depending upon the degree of energy absorption by the microstructure of a medium, shear flow, craze or crack may occur. If craze occurs first, then the transition from craze to crack is likely to be highly nonlinear. Results are important in studying the time-dependent strength and fracture behavior of polymeric and composite systems. By averaging all the microscopic

behavior specific in each molecular orientation, a fracture criterion may be established to analyze the time and deformation dependent breaking strength of an oriented polymer solid. Utilizing spherical functions and the double Fourier series expansion, the statistical microscopic behavior in the vicinity of a point in an oriented medium may be converted into several symmetric tensorial terms. Then the time-to-break can be synthesized and incorporated in calculating the macroscopic behavior. By taking into account the individual values of the directional fraction of integrity, the fracture time as well as the most probable direction of fracture initiation within any volume element in the medium can be predicted. However, results thus obtained governs only the localized behavior of a material. For a layered composite system, the interactions among craze-crack regions must also be determined. Perhaps a joint distribution function of the characteristic parameters can be introduced to obtain the final analytical result of the strength and fracture of a composite system. In addition, since the material systems are viscoelastic, measurements of temperature fields in and around a craze-crack system are extremely important in connecting the properties of the microstructure and the analysis of the energy dissipation of the macromechanical behavior.

APPENDIX

Substituting Equation (42) into (47) and (48), yields

$$\int_b^a \Phi dx = \frac{1}{\pi}\{[(\sigma_2-\sigma_1)a\sqrt{c^2-a^2}$$

$$+ \sigma_1 b\sqrt{c^2-b^2}\,](\sin^{-1}\frac{a}{c} - \sin^{-1}\frac{b}{c})$$

$$+\frac{1}{2}(2\sigma_1-\sigma_2)(a^2+b^2)\ln\frac{a\sqrt{c^2-b^2}-b\sqrt{c^2-a^2}}{a\sqrt{c^2-b^2}+b\sqrt{c^2-a^2}}$$

$$-(2\sigma_1-\sigma_2)ab\,\ln\frac{\sqrt{c^2-b^2}-\sqrt{c^2-a^2}}{\sqrt{c^2-b^2}+\sqrt{c^2-a^2}}$$

$$+2(\sigma_1-\sigma_2)a^2\ln\frac{a}{c}+2\sigma_1 b^2\ln\frac{b}{c}\}, \qquad (A1)$$

$$\int_a^c \Phi dx = \frac{1}{\pi}\{[(\sigma_2-\sigma_1)\,a\sqrt{c^2-a^2}+\sigma_1 b\sqrt{c^2-b^2}\,]\cos^{-1}\frac{a}{c}$$

$$-\frac{1}{2}\sigma_1(a^2+b^2)\ln\frac{a\sqrt{c^2-b^2}-b\sqrt{c^2-a^2}}{a\sqrt{c^2-b^2}+b\sqrt{c^2-a^2}}$$

$$+ab\sigma_1\,\ln\frac{\sqrt{c^2-b^2}-\sqrt{c^2-a^2}}{\sqrt{c^2-b^2}+\sqrt{c^2-a^2}}$$

$$+2(\sigma_2-\sigma_1)a^2\ln\frac{a}{c}\}. \qquad (A2)$$

Differentiating (A1) and (A2) yields

$$\frac{\partial\Phi_{ba}}{\partial a} = \frac{1}{\pi}[(\sigma_2-\sigma_1)(\sin^{-1}\frac{a}{c}-\sin^{-1}\frac{b}{c})\frac{c^2-2a^2}{\sqrt{c^2-a^2}}$$

$$+ (\sigma_2-\sigma_1)(b\frac{\sqrt{c^2-b^2}}{\sqrt{c^2-a^2}} - a - 4a\ln\frac{a}{c})$$

$$-(\sigma_2-2\sigma_1)(a\,\ln\frac{a\sqrt{c^2-b^2}-b\sqrt{c^2-a^2}}{a\sqrt{c^2-b^2}+b\sqrt{c^2-a^2}}$$

$$-b\,\ln\frac{\sqrt{c^2-b^2}-\sqrt{c^2-a^2}}{\sqrt{c^2-b^2}+\sqrt{c^2-a^2}})], \qquad (A3)$$

$$\frac{\partial\Phi_{ba}}{\partial b} = \frac{1}{\pi}[\sigma_1(\sin^{-1}\frac{a}{c}-\sin^{-1}\frac{b}{c})\frac{c^2-2b^2}{\sqrt{c^2-b^2}}$$

$$-\sigma_1(a\frac{\sqrt{c^2-a^2}}{\sqrt{c^2-b^2}} - b - 4b\ln\frac{b}{c})$$

$$-(\sigma_2-2\sigma_1)(b\,\ln\frac{a\sqrt{c^2-b^2}-b\sqrt{c^2-a^2}}{a\sqrt{c^2-b^2}+b\sqrt{c^2-a^2}}$$

$$-a\,\ln\frac{\sqrt{c^2-b^2}-\sqrt{c^2-a^2}}{\sqrt{c^2-b^2}+\sqrt{c^2-a^2}})], \qquad (A4)$$

$$\frac{\partial\Phi_{ba}}{\partial c} = \frac{1}{\pi}\{[(\sigma_2-\sigma_1)\frac{a}{\sqrt{c^2-a^2}}+\sigma_1\frac{b}{\sqrt{c^2-b^2}}\,]\cdot$$

$$(\sin^{-1}\frac{a}{c}-\sin^{-1}\frac{b}{c})c$$

$$+(\sigma_2-\sigma_1)\frac{a^2}{c}-\sigma_1\frac{b^2}{c}+\frac{ab}{c\sqrt{c^2-a^2}\sqrt{c^2-b^2}}\cdot$$

$$[(\sigma_2-\sigma_1)b^2-\sigma_1 a^2-(\sigma_2-2\sigma_1)c^2]\}, \qquad (A5)$$

$$\frac{\partial\Phi_{ac}}{\partial b} = \frac{1}{\pi}[(\sigma_2-\sigma_1)(\frac{c^2-2a^2}{\sqrt{c^2-a^2}}\cos^{-1}\frac{a}{c}+a+4a\ln\frac{a}{c})$$

$$-\sigma_1 a\,\ln\frac{a\sqrt{c^2-b^2}-b\sqrt{c^2-a^2}}{a\sqrt{c^2-b^2}+b\sqrt{c^2-a^2}}$$

$$+\sigma_1 b\,\ln\frac{\sqrt{c^2-b^2}-\sqrt{c^2-a^2}}{\sqrt{c^2-b^2}+\sqrt{c^2-a^2}}, \qquad (A6)$$

$$\frac{\partial\Phi_{ac}}{\partial b} = \frac{\sigma_1}{\pi}(\frac{c^2-2b^2}{\sqrt{c^2-b^2}}\cos^{-1}\frac{a}{c}+a\frac{\sqrt{c^2-a^2}}{\sqrt{c^2-b^2}}$$

$$-b\,\ln\frac{a\sqrt{c^2-b^2}-b\sqrt{c^2-a^2}}{a\sqrt{c^2-b^2}+b\sqrt{c^2-a^2}}$$

$$+a\,\ln\frac{\sqrt{c^2-b^2}-\sqrt{c^2-a^2}}{\sqrt{c^2-b^2}+\sqrt{c^2-a^2}}), \qquad (A7)$$

$$\frac{\partial\Phi_{ac}}{\partial c} = \frac{1}{\pi}\{[(\sigma_2-\sigma_1)\frac{a}{\sqrt{c^2-a^2}}+\sigma_1\frac{b}{\sqrt{c^2-b^2}}\,]c\cos^{-1}\frac{a}{c}$$

$$-(\sigma_2-\sigma_1)\frac{a^2}{c}-\sigma_1\frac{ab\sqrt{c^2-a^2}}{c\sqrt{c^2-b^2}}\}. \qquad (A8)$$

ACKNOWLEDGEMENTS

REFERENCES

1. Hsiao, C. C. and Sauer, J. A., "On Crazing of Linear High Polymers," Journal of Applied Physics, Vol. 21, No. 11, Nov. 1950, pp. 1071-1083.

2. Knight, A. D., "Stress Crazing of Transparent Plastics. Computed Stresses at a Nonvoid Craze Mark," Journal of Polymer Science, Part A, Vol. 3, 1965, pp. 1845-1857.

3. Warren, W. A., "Stress and Displacement Fields at the Tip of a Craze Containing a Crack," Polymer Engineering and Science, Vol. 24, No. 10, July 1984, pp. 814-819.

4. Walton, J. R. and Weitsman, Y., "Deformations and Stress Intensities Due to a Craze in an Extended Elastic Material," Journal of Applied Mechanics, Vol. 51, March 1984, pp. 84-92.

5. Williams, M. L., "Initiation and Growth of Viscoelastic Fracture," International Journal of Fracture Mechanics, Vol. 1, No. 4, 1965, pp. 292-310.

6. Willis, J. R., "Crack Propagation in Viscoelastic Media," Journal of Mechanics and Physics of Solids, Vol. 15, No. 4, 1967, pp. 229-240.

7. Graham, G. A. C., "The Correspondence Principle of Linear Viscoelasticity Theory for Mixed Boundary Value Problems Involving Time-Dependent Boundary Regions," Quarterly Applied Mathematics, Vol. 26, No. 2, 1968, pp. 167-174. "Two Extending Crack Problems in Linear Viscoelasticity Theory," Vol. 27, No. 4, 1969, pp. 497-507.

8. McCartney, L. N., "Crack Propagation, Resulting from a Monotonic Increasing Applied Stress, in a Linear Viscoelastic Material," International Journal of Fracture, Vol. 13, No. 5, Oct. 1977, pp. 641-654.

9. Schapery, R. A., "A Theory of Crack Initiation and Growth in Viscoelastic Media," International Journal of Fracture, I. Theoretical Development, Vol. 11, No. 1, Feb. 1975, pp. 141-159. II. Approximate Methods of Analysis, Vol. 11, No. 3, June 1975, pp. 369-388. III. Analysis of Continuous Growth, Vol. 11, No. 4, Aug. 1975, pp. 549-562.

10. Schapery, R. A., "A Method for Predicting Crack Growth in Nonhomogeneous Viscoelastic Media," International Journal of Fracture, Vol. 14, No. 3, June 1978, pp. 293-309. "Correspondence Principles and a Generalized J Integral for Large Deformation and Fracture Analysis of Viscoelastic Media," Vol. 25, 1984, pp. 195-223.

11. Hsiao, C. C. and Moghe, S. R., "Characterization of Random Microstructural Systems," Proceedings of the 1969 International Conference on Structure. Solid Mechanics and Engineering Design in Civil Engineering Materials, Southampton, England, John Wiley, London, Part I, 1971, pp. 95-103.

12. Chern, S. S. and Hsiao, C. C., "A Generalized Time-Dependent Theory on Craze Initiation in Viscoelastic Media," Journal of Applied Physics, Vol. 57, No. 6, March 1985, pp. 1823-1834.

13. Hsiao, C. C., "Fracture," Physics Today, Vol. 19, No. 3, March, 1966, pp. 49-53.

14. Kausch von Schmeling, H. H., Mohge, S. R. and Hsiao, C. C., "Influence of Reforming Processes on the Fracture Strength of Solids," Journal of Applied Physics, Vol. 38, No. 1, Jan. 1967, pp. 201-204.

15. Moghe, S. R., Kawatate, K., Cheung, J. E. and Hsiao, C. C., "Mechanical Breakdown of Oriented Solids under Time Dependent Loads," Proceedings of the Fifth International Congress on Rheology, Vol. 1, Oct. 7-11, 1968, Kyoto, Japan, 1969, pp. 595-606.

16. Kuksenko, V. S. and Tamuzs, V. P., Fracture Micromechanics of Polymer Materials, Martinus Nijhoff Publishers, Hague, Boston, London, 1981, Chapter 7.

17. Chern, S. S. and Hsiao, C. C., "A Time Dependent Theory of Crazing Behavior in Polymers," Journal of Applied Physics, Vol. 53, No. 10, Oct. 1982, pp. 6541-6551.

18. Kramer, E. M., "Craze Fibril Formation and Breakdown," Polymer Engineering and Science, Vol. 24, No. 10, July 1984, pp. 761-769.

19. Doll, W., "Kinetics of Crack Tip Craze Zone Before and During Fracture," Polymer Engineering and Science, Vol. 24, No. 10, July 1984, pp. 798-808.

20. Verheulpen-Heymans, N., "Craze Failure by Midrib Creep," Polymer Engineering and Science, Vol. 24, No. 10, July 1984, pp. 809-813.

21. Williams, J. G., "Modelling Crack Tip Failure Mechanisms in Polymers," Metal Science, Aug-Sept. 1980, pp. 344-350.

22. Chan, T., Donald, A. M., Kramer, E. J., "Film Thickness Effects on Craze Micromechanics," Journal of Material Science, Vol. 16, 1981, pp. 676-686.

23. Zhang, Z. D., Chern, S. S. and Hsiao, C. C., "Propagation of Crazing in Viscoelastic Media," Journal of Applied Physics, Vol. 54, No. 10, Oct. 1983, pp. 5568-5576.

ANALYZING POLYMER CRAZING AS QUASIFRACTURE

B. N. Sun and C. C. Hsiao

Dept. of Aerospace Engineering and Mechanics

University of Minnesota

Minneapolis, Minnesota

ABSTRACT

This paper deals with a viscoelastic boundary element method for analyzing a polymer quasifracture termed earlier as a craze in polymers. A time dependent boundary stiffness is considered on the quasifracture envelope surface. The viscoelastic property of the glassy polymer is represented by a generalized Kelvin model with multiple retardation times. According to the linear viscoelastic correspondence principle, the associated elasticity solution can be solved by applying the general integral boundary element method. Then the viscoelastic solution in the time domain can be obtained by applying collocation Laplace inversion transformation. Using these methods, the quasifracture problem composed of an isolated craze opening with time dependent stiffness traction in a stressed rectangular plate is analyzed. The displacement profile and the stress distribution around the craze envelope surface are computed.

INTRODUCTION

The craze or quasifracture behavior of glassy polymers has been studied by many scientists using theoretical and/or experimental methods recently [1,2,3]. Only a few papers reported the linear elastic quasifracture behavior using numerical methods. L. Bevan [4] applied both the elastic finite-element method and boundary-element method with linear boundary condition for investigating the craze problem. Recently, using the nonlinear finite element method, the stress distribution around the envelope surface and the displacement profile associated with a craze has been reported [5]. However, since the boundary element method has currently become a powerful technique for solving boundary value problems including some nonlinear ones, it is worthy of utilizing, as it has several advantages over the finite element method. The number of unknowns in the calculating system depends only on the boundary discretization rather than upon the discretization of the whole volume of the material body as in the finite element method. The singular kernels in the integral equations weigh the unknown quantities near a singular point more heavily as compared with those far away and the resultant matrices are generally well behaved. The physical quantities obtained by differentiation of the primary variables such as the stresses obtained from displacements are determined pointwise inside and on the body. Thus there is less chance to have discontinuities. This is especially important in problems having viscoelastic deformations and, in particular, viscoelastic fracture mechanics problems [6]. In addition, this method takes less computing time and yields greater accuracy as compared with those problems analyzed using the finite element method under somewhat similar situations. Therefore, in the case wherein highly localized

stresses may exist, more elements can be introduced so that any possible sin-gularities will not be suppressed by the analysis. As the quasifracture beha-vior of crazing is important for studying engineering plastics and polymer com-posites, in this paper, a viscoelastic boundary element method for analyzing the polymer quasifracture and determining the displacement field has been dev-eloped. In this attempt emphasis is placed on the procedural development of the method. Actually measured displacement field obtained earlier has been employed [3] in the computation.

It is well known that glassy polymers behave viscoelastically. Using the correspondence principle in linear theory of viscoelasticity, the quasifracture behavior of a polymer can be calculated from the solution of an associated elasticity problem by means of numerical method, then inversion yields the required time dependent response. Therefore, in this paper the boundary ele-ment method is applied to solve the associated elasticity problem in the Laplace domain. By applying the numerical Laplace inversion technique devel-oped by Schapery [7] and Cost [8], the associated elasticity solution can be transformed from the Laplace domain back into the time domain. There are sev-eral reports dealing with the use of the viscoelastic boundary element method. For simple specific viscoelastic models, Takashi Kusama and Yasushi Mitsui [9] developed an improved collocation method and applied the boundary element method to solve a Kelvin viscoelastic model. Rizzo and Shippy [10] used the direct boundary integral method to solve a standard linear viscoelastic model. Wang and Crouch [11] applied the displacement discontinuity boundary element method and collocation inversion technique to solve a rock mechanics problem represented by a Burgers model. In this paper the general boundary element method together with the collocation inversion technique is used to solve an isolated quasifracture having a generalized Kelvin model behavior with multiple

retardation times. In using such a method the prescribed boundary condition is either the displacement or the traction condition. For a quasifracture problem the boundary condition on the craze envelope surface is prescribed in a stiffness form. By considering the molecular orientation mechanism [12] of the craze fibril domains, the boundary displacement of a craze envelope surface may be represented by a convolution integral. Then the displacement field and the stress distribution along a craze surface envelope can be calculated in several time steps. It is interesting to show that the calculated resulting stress distribution along the craze envelope surface did not change very much with respect to initial zero time and several hundred hours.

FUNDAMENTAL BOUNDARY VALUE PROBLEM

The governing equations for the quasifracture boundary value problem are the equilibrium equations in terms of the stress components σ_{ij}, relations between displacements u_i and strain components ε_{ij} together with a set of constitutive equations. The stress and displacement fields must satisfy the prescribed boundary conditions on the craze envelope surface and other boundaries. They are, in a rectangular coordinate system $(0-x_1,x_2,x_3)$:

$$\sigma_{ij,j}(x_1,x_3,t) = 0, \tag{1}$$

$$\varepsilon_{ij}(x_1,x_3,t) = \frac{1}{2}[u_{i,j}(x_1,x_3,t) + u_{j,i}(x_1,x_3,t)]. \tag{2}$$

The constitutive equations can be written in integral form as:

$$e_{ij}(t) = \int_{-\infty}^{t} J(t-\tau) \frac{\partial S_{ij}(\tau)}{\partial \tau} d\tau, \tag{3}$$

$$\epsilon_{kk}(t) = \int_{-\infty}^{t} B(t-\tau) \frac{\partial \sigma_{kk}(\tau)}{\partial \tau} d\tau, \tag{4}$$

where $J(t)$ and $B(t)$ are respectively the creep compliance functions in shear and isotropic dilation or bulk creep compliance; σ_{kk} and ϵ_{kk} are respectively the hydrostatic stresses and strains by implying the summation convention. S_{ij} and e_{ij} are respectively the deviatoric components of stress tensor σ_{ij} and strain tensor ϵ_{ij} and are related with other stress and strain components as follows:

$$S_{ij} = \sigma_{ij} - \frac{1}{3} \delta_{ij}\sigma_{kk}. \tag{5}$$

$$e_{ij} = \epsilon_{ij} - \frac{1}{3} \delta_{ij}\epsilon_{kk}. \tag{6}$$

where δ_{ij} are delta functions.

In a linear viscoelastic polymer, a very good approximation [3,13,14] for the tensile creep compliance $D(t)$ is obtainable using a generalized Kelvin model composed of a series of Voigt elements or simply it can be mathematically represented in the following form:

$$D(t) = D_0 + \sum_{n=1}^{n} D_n \left[1 - \exp(-\frac{t}{\tau_n}) \right], \tag{7}$$

where D_e and D_η are constants and τ_η are discrete retardation times. Now if one adopts the notation and definition that

$$\overline{f}(x_1,x_3,s) = \int_0^\infty f(x_1,x_3,t)e^{-st} \, dt, \tag{8}$$

where $\overline{f}(x_1,x_3,s)$ is the Laplace transform of the time dependent function $f(x_1,x_3,t)$ with s as the Laplace parameter, then it can be shown that the shear and bulk creep compliance functions can be obtained through Laplace inversion:

$$J(t) = L^{-1}(\overline{J}(s)) = L^{-1}[(1 + s\overline{v}(s))\overline{J}(s)] , \tag{9}$$

$$B(t) = L^{-1}(\overline{B}(s)) = L^{-1}[(1 - 2s\overline{v}(s))\overline{B}(s)] , \tag{10}$$

where $\overline{v}(s)$ is the Laplace transform of the time dependent strain ratio. It is to be noted that in analyzing a problem involving the time dependent viscoelasticity, $v(t)$ is time dependent. The quantity Poisson's ratio in classical theory of elasticity is meaningless in viscoelastic behavior, thus $v(t)$ is termed strain ratio. Experimental results [15] have shown that the strain ratio $v(t)$ became approximately a constant for long creep times. With this information, the viscoelastic tensile relaxation modulus function $E(t)$ can be shown as:

$$E(t) = L^{-1}\left[\frac{1}{s^2\overline{D}(s)}\right] = L^{-1}\left[\frac{1}{s(D_0 + \sum\limits_{\eta=1}^{n} D_\eta \frac{1}{\tau_\eta s+1})}\right]. \tag{11}$$

In the craze region, oriented molecular domains and voids are formed as shown schematically in Fig. 1. Since the domains are composed of groups of connected fibrils of molecules, they bear load and are subjected to large deformations. When a craze elongates its displacement field in the direction of stressing also increases. While a part of the contribution of the displacement field is because of the creeping of the fibril-domains, the major contribution comes as a result of the drawing of the molecules from the bulk of the polymer. This drawing mechanism coupled with a simultaneous neckdown of the fiber domains dominates the local well known crazing behavior composed of molecular orientation mechanism and formation of porosities. A local strain field ϵ ($-1 < \epsilon < \infty$ defined as $\lambda - 1$ where λ is the draw ratio) identifies the degree of molecular orientation termed the orientation strain and has been found essentially constant [2, 3, 16] throughout the craze length as it is intimately associated with the natural draw ratio of the polymer. During the process of deformation, the stress state of an individual fibril domain is considered as uniaxial tension. Under a uniaxial stress $\sigma_{33}(x_1, t)$, a corresponding small strain $\epsilon_{33}(x_1, t) \ll \epsilon(x_1, t)$, the orientation strain, of a fibril domain will occur. The relationship between the small strain and the tensile stress of each fibril domain at x_1 is:

$$\sigma_{33}(x_1, t) = \int_{-\infty}^{t} E_f(x_1, t - \tau) \frac{\partial \epsilon_{33}(x_1, \tau)}{\partial \tau} d\tau, \qquad \text{on } x_1 \leq c, \ x_3 = 0, \tag{12}$$

where $E_f(t)$ is the viscoelastic tensile relaxation modulus of the fibril domain while the orientation strain ε contributes no additional stress. In preparation for computation using boundary element method the traction $T_3(x_1,t)$ acting on the craze envelope at x_1 may be written as follows:

$$T_3(x_1,t) = \int_{-\infty}^{t} K(x_1,t-\tau) \frac{\partial U_3(x_1,\tau)}{\partial \tau} d\tau$$

$$= K(x_1,0)\, U_3(x_1,t) + \int_{0}^{t} \dot{K}(x_1,t-\tau)\, U_3(x_1,\tau)\, d\tau, \qquad \text{on } x_1 \leq c, \ x_3 = 0, \qquad (13)$$

where $U_3(x_1,t)$ is the opening displacement measured from the horizontal center line of symmetry of the craze corresponding to $\varepsilon_{33}(x_1,t)$ at the boundary of the craze envelope at x_1 [2] as the thickness of the primordial layer is small as compared with U_3. By writing

$$K(x_1,t) = \frac{E_f(x_1,t)}{U_3(x_1,0)}, \qquad (0 \leq t < \infty), \qquad (14)$$

then it becomes the stiffness per unit area of a craze fibril domain. $K(x_1,0) = K(x_1,t)\big|_{t=0}$ is the initial stiffness at x_1. Now we use the convolution integral relationship (13) as the boundary condition on the craze envelope. The tensile creep compliance $D_f(t)$ of a fibril domain can be found. By referring to the molecular orientation theory [12], the tensile relaxation modulus $E_f(\varepsilon)$ of a fibril domain may be represented as follows:

$$E_f(\epsilon) = C(\epsilon)E \qquad (15)$$

where, as stated before, ϵ, the orientation strain, is essentially a constant, thus, $C(\epsilon)$ being a function of the orientation strain is also a constant and E is the modulus of elasticity of the original polymer medium. Therefore, if the time dependency is introduced as given in the following equation:

$$E_f(\epsilon,t) = C(\epsilon)E(t), \qquad (16)$$

both the nature of molecular orientation and the time dependent viscoelastic behavior of the moduli are preserved. In the Laplace domain, treat $C(\epsilon)$ as constant, then

$$\overline{E}_f(\epsilon,s) = C(\epsilon)\overline{E}(s), \qquad (17)$$

and

$$s^2\overline{E}(s)\overline{D}(s) = 1. \qquad (18)$$

For individual fibril domains a similar relationship may be written as

$$s^2\overline{E}_f(s)\overline{D}_f(s) = 1, \qquad (19)$$

where $\overline{D}_f(s)$ is the tensile creep compliance function of the fibril domain in the Laplace s-domain. Solving for $\overline{D}_f(s)$, one gets

$$\overline{D}_f(s) = C^{-1}(\epsilon)[s^2\overline{E}(s)]^{-1}, \qquad (20)$$

or

$$\overline{D}_f(s) = C^{-1}(\epsilon)\overline{D}(s). \tag{21}$$

Thus after inversion

$$D_f(t) = C^{-1}(\epsilon)D(t). \tag{22}$$

At position x_1, let us write

$$D_f(x_1,t) = C^{-1}(x_1,\epsilon)D(t) = C^{-1}(x_1,\epsilon)\{D_0 + \sum_{\eta=1}^{n} D_\eta[1 - \exp(-t/\tau_\eta)]\}. \tag{23}$$

where

$$C^{-1}(x_1,\epsilon) = D_f(x_1,0)/D_0 \tag{24}$$

is a spatial parameter, then the stiffness becomes:

$$K(x_1,t) = L^{-1}\left[\frac{\overline{E}_f(x_1,s)}{U_3(x_1,0)}\right] = L^{-1}\left[\frac{K(x_1,0)D_0}{s^2\overline{D}(s)}\right]. \tag{25}$$

And the traction $T_3(x_1,t)$ acting on the craze envelope surface equals:

$$T_3(x_1,t) = L^{-1}[s\overline{K}(x_1,s)\overline{U}_3(x_1,s)]. \tag{26}$$

According to the correspondence principle in linear viscoelasticity, we can transfer the boundary value problem of quasifracture into the s-domain merely by replacing the elastic parameters by their corresponding time dependent viscoelastic parameters in the Laplace domain s as follows:

$$E \rightarrow s\overline{E}(s),$$

$$K \rightarrow K(x_i,0)D_o/s^2\overline{D}(x_i,s),$$

(27)

$$(T_i)_o \rightarrow (\overline{T}_i)_o(s) = (T_i)_o/s,$$

$$(U_i)_o \rightarrow (\overline{U}_i)_o(s) = (U_i)_o/s,$$

where $(T_i)_o$ and $(U_i)_o$ are respectively the prescribed constant boundary traction and displacement at point i. Once the associated elasticity solution is obtained, then the Laplace numerical inversion will yield the time dependent solution of the problem.

CALCULATING PROCEDURE

In order to solve the associated elasticity problem, the general integral boundary element method may be applied. The detailed investigation of these methods and others may be found in the literature [17-19]. For simplicity only one approach is utilized and the basic formulation for the linear elasticity problem is described here. In the two-dimensional elastic continuum R with boundary Γ, which is assumed to be isotropic without body force, the gov-

erning equation may be obtained from pages 125 and 126 of reference [17] as follows:

$$C^i U_\ell^i + \int_\Gamma T^*_{\ell k} U_k \, d\Gamma = \int_\Gamma U^*_{\ell k} T_k \, d\Gamma, \quad (k, \ell = 1 \text{ or } 3) \tag{28}$$

where $C^i = 1/2$ for point i when it becomes a boundary point on a smooth boundary, $U^*_{\ell k}$ is the displacement in the k direction due to a unit force acting in the ℓ direction at point i, U_k is the displacement at any point on the boundary Γ in the k direction, T_k is the traction at any point on the boundary Γ in the k direciton, and $T^*_{\ell k}$ is the traction in the k direction due to a unit force acting in the ℓ direction at point i. The fundamental solutions for the two dimensional isotropic plane strain problem are easily written following the equations given on pages 126 and 141 of reference [17]. They are

$$U^*_{\ell k} = \frac{1}{8\pi G(1 - \nu)} \left[(3 - 4\nu)\delta_{\ell k} \ln(\frac{1}{r}) + \frac{\partial r}{\partial x_\ell} \cdot \frac{\partial r}{\partial x_k} \right],$$

$$\tag{29}$$

$$T^*_{\ell k} = \frac{-1}{4\pi(1 - \nu)r} \left\{ \frac{\partial r}{\partial n}[(1 - 2\nu)\delta_{\ell k} + 2 \frac{\partial r}{\partial x_\ell} \frac{\partial r}{\partial x_k}] - (1 - 2\nu) [\frac{\partial r}{\partial x_\ell} n_k - \frac{\partial r}{\partial x_k} n_\ell] \right\},$$

where G, ν are elastic shear modulus and Poisson's ratio respectively and n_ℓ is the outward normal to the boundary and r is the distance from the load point to the point under consideration. Equation (29) is known as the Kelvin's singular solution due to a point load in an infinite ̲lastic medium.

At first, the boundary Γ was divided into N elements with assumed constant values of U_k and T_k in each element. By applying the viscoelastic cor-

respondence principle, the following equations are obtained in the Laplace domain:

$$C^i \overline{U}_\ell^i + \sum_{q=1}^{N} \int_{\Gamma_q} \overline{T}_{\ell k}^* \overline{U}_k \, d\Gamma = \sum_{q=1}^{N} \int_{\Gamma_q} \overline{U}_{\ell k}^* \overline{T}_k \, d\Gamma, \qquad \begin{array}{l} (k, \ell = 1 \text{ or } 3) \\ (q = 1, 2, \ldots, N) \end{array} \qquad (30)$$

As shown above there are 2N simultaneous algebraic equations. When 2N boundary tractions and boundary displacements are given another 2N unknown boundary tractions and boundary displacements can be obtained. For some boundary elements, beginning α, say, such as Γ_q ($q = \alpha, \ldots N$), on which the stiffness boundary condition was prescribed. Equation (30) will become as follows:

$$C^i \overline{U}_\ell^i + \sum_{q=1}^{\alpha-1} \int_{\Gamma_q} \overline{T}_{\ell k}^* \overline{U}_k \, d\Gamma + \sum_{q=\alpha}^{N} \int_{\Gamma_q} (\overline{T}_{\ell k}^* - K_k \overline{U}_{\ell k}^*) \overline{U}_k \, d\Gamma =$$

$$= \sum_{q=1}^{\alpha-1} \int_{\Gamma_q} \overline{U}_{\ell k}^* \overline{T}_k \, d\Gamma, \qquad (q = 1, 2 \ldots \ldots \alpha \ldots \ldots N) \qquad (31)$$

By solving the above simultaneous algebraic equations, we can obtain the values $\overline{U}_k$ and $\overline{T}_k$ successively for discrete values in the Laplace domain. Based upon the thermodynamic principle, Schapery [7] developed a collocation method of numerical Laplace transform inversion. This method shows that the components of stress and displacement at any point can be represented by a series F(t) defined as follows:

$$F(t) = C_1 + C_2 t + \sum_{m=1}^{M} A_m e^{-b_m t}, \tag{32}$$

where C_1, C_2, A_m and b_m are constants. Taking the Laplace transform of Equation (32) and multiplying by the transformation parameter s gives:

$$s\overline{F}(s) = C_1 + \frac{C_2}{s} + \sum_{m=1}^{M} \frac{A_m}{1 + b_m/s_j}. \tag{33}$$

When time t goes to infinity the function $F(t)$ should be finite. Therefore, the constant C_2 is chosen to be zero. In order to determine the constants in this equation a value for M and a sequence of values of s must be selected, i.e.:

$$s = s_\beta \quad , \qquad (\beta=1,2,\cdots\cdots,M+1), \tag{34}$$

Based upon Schapery's suggestion, the relationship between s and t is $s = 1/2t$. The M values of b_m are taken to be the first M+1 values of s. Then Equation (33) can be written:

$$s_\beta \overline{F}(s_\beta) = C_1 + \sum_{m=1}^{M} \frac{A_m}{1 + b_m/s_\beta} , \qquad (\beta = 1, 2,\cdots\cdots M, M+1), \tag{35}$$

which is a set of M+1 linear algebraic equations with M+1 unknowns C_1 and A_m solvable using standard procedures. The guidelines for selecting the discrete

values of s can be found in Rizzo and Shippy [10].

BEHAVIOR OF A CRAZE

According to the aforementioned theory and method, an illustration is provided by calculating the displacement field in the neighborhood of a hole in a linear viscoelastic infinite plate. The load applied was expressed as a step function. The contour of the circular hole has been divided into 24 boundary elements as shown in Fig. 2. The radial displacements calculated by either the viscoelastic boundary element method or an analytical solution are shown in Fig. 3. The radius of the hole is 3 m. The applied internal pressure is 100 MN/m². For linear viscoelastic behavior the tensile creep compliances of the material was represented by a generalized Kelvin model with multiple retardation times, as shown below:

$$D_0 = 0.238 \times 10^{-3} \text{ m}^2/\text{MN}, \qquad \nu = 0.33,$$

$$D_1 = 0.071 \times 10^{-3} \text{ m}^2/\text{MN}, \qquad \tau_1 = 1 \quad \text{hour},$$

$$D_2 = 0.062 \times 10^{-3} \text{ m}^2/\text{MN}, \qquad \tau_2 = 10 \quad \text{hours},$$

$$D_3 = 0.045 \times 10^{-3} \text{ m}^2/\text{MN}, \qquad \tau_3 = 80 \quad \text{hours},$$

$$D_4 = 0.031 \times 10^{-3} \text{ m}^2/\text{MN}, \qquad \tau_4 = 110 \text{ hours}.$$

As seen in Fig. 3, the computed data by the viscoelastic boundary element method produced excellent agreement with the analytical results obtained by transforming the classical elasticity solution of a circular hole in an infinite plate into a time dependent solution in linear viscoelasticity using the well known correspondence principle.

Now for studying the quasifracture, an idealized symmetrical craze in a constant stress field has been considered. The craze basic structure was rep-

resented by a slit with fiber domains distributed along the craze envelope boundary. The distance between the top and the bottom craze envelopes has been referred to as the craze opening displacement measured from the center of symmetry. The stress acting on the interface of the craze was referred to as the craze envelope stress. The total craze length considered was 2 mm thus c = 1 mm, which is usually referred to as the craze length measured from the center of a craze. The width of plate was B = 11.2 mm and the length of the plate was L = 14 mm with unit thickness throughout. Because of symmetry, a quarter of the plate containing an isolated quasifracture was divided into 58 boundary elements as shown in Fig. 4. The properties of the bulk material was again represented by a generalized Kelvin model. The tensile creep compliances D_m, retardation times τ_m were given as before. The shape of the applied stress p_0 was a unit step function $H(t)$ modified to 42 N/mm^2. The boundary conditions used on the plate are:

$$T_3(x_1,t) = \int_0^t K(x_1,t-\tau) \frac{\partial U_3(x_1,\tau)}{\partial \tau} dt$$

$$(x_1 \leq c, \quad x_3 = 0), \qquad (36)$$

$$T_1(x_1,t) = 0$$

$$U_3(x_1,t) = 0$$

$$(c \leq x_1 \leq B, \quad x_3 = 0), \qquad (37)$$

$$T_1(x_1,t) = 0$$

$$T_1(x_3,t) = 0$$

$$(x_1 = B, \quad 0 \leq x_3 \leq L), \qquad (38)$$

$$T_3(x_3,t) = 0$$

$$T_1(x_1,t) = 0$$

$$(0 \le x_1 \le B, \quad x_3 = L), \qquad (39)$$

$$T_3(x_1,t) = p_0 H(t)$$

$$U_1(x_3,t) = 0$$

$$(x_1 = 0, \quad 0 \le x_3 \le L). \qquad (40)$$

$$T_3(x_3,t) = 0$$

Initially by using the finite element method and considering the molecular orientation of the fibril domains in the quasifracture [4], the initial instantaneous craze opening displacement $U_3(x_1,0)$ and the craze envelope stress $\sigma_C(x_1,0)$ have been calculated. They agreed fairly well with the experimental results. Subsequently the instantaneous stiffness $K(x_1,0)$ was calculated and $K(x_1,t)$ determined from Expression (25). In applying viscoelastic boundary element method, the values of s-parameter were selected ranging from 10^{-3}, 10^{-2}, 10^{-1}, 10^0, 10^1, to 10^2 and time t was chosen as 1/25 as given earlier [7-10]. Fig. 5 shows the opening displacement $U_3 = w$ between the quasifracture envelope surfaces versus the distance from the center of craze for various times corresponding to 500, 50, 5 and 0 hours. It is seen that the quasifracture opening displacement increases as time increases. The rate of increment is relatively high from 0 to 50 hours. Beyond 50 hours, the opening displacement changes slowly. However, it is interesting to find out that the stress distribution has maintained its constant value as shown in Fig. 6. These results indicate that the craze quasifracture behavior can be successfully analyzed using this viscoelastic boundary element method.

ACKNOWLEDGEMENTS

REFERENCES

1. S.S. Chern and C.C. Hsiao, J. Appl. Phys. 52, 5994 (1981).

2. S.S. Chern and C.C. Hsiao, J. Appl. Phys. 53, 6541 (1982).

3. B.D. Lauterwasser and E.J. Kramer, Philos. Mag. A, 39, 469 (1979); Philos. Bull. 3, 565 (1980).

4. L. Bevan, J. Polymer Sci. Phys. 19, 1759 (1981); J. of Appl. Poly. Sci. 27, 4263 (1982).

5. B.N. Sun and C.C. Hsiao, Journal of Applied Physics, 57, 170 (1985).

6. S. Mukherjee, Boundary Element Methods in Creep and Fracture, Applied Science Publishers, London, (1982).

7. R.A. Schapery, U.S. National Congress of Appl. Mech. 1075 (1961).

8. T.L. Cost, AIAA Journal 2, 2157 (1964).

9. Takashi Kusama and Yasushi Mitsui, Appl. Math. Modelling 6, 285 (1982).

10. F.J. Rizzo, D.J. Shippy, SIAM J. Appl. Math. 21, 321 (1971).

11. Y.G. Wang, S.L. Crouch, 23rd U.S. Symposium Rock Mechanics, Berkeley, California, 704 (1982).

12. C.C. Hsiao, J. Appl. Phys., 30, 1942 (1959); J. Polymer Sci. 44, 71 (1960); Section IVC, Fracture Processes in Polymeric Solids (ed. B. Rosen), Interscience (John Wiley), 529 (1964).

13. H.H. Kausch and M. Dettermaier, Polym. Bull. 3, 565 (1980).

14. A.J. Staverman, F. Schwarzl, Chap. 1, Die Physik der Hochpolymeren, (ed. H.A. Stuart) Springer, Berlin , 1 (1965).

15. Z. Rigbi, Applied Polymer Symposia, 1 (1967).

16. A.M. Donald, E.J. Kramer and R.A. Bubeck, J. Polymer Sci.--Polymer Phys. 20, 1129 (1982).

17.   *C.A. Brebbia and S. Walker*, The Boundary Element Techniques in Engineering, Newnes-Butterworths, 120 (1980).

18.   P. K. Banerjee and R. Butterfield, Boundary Element Methods in Engineering Science, McGraw-Hill (UK), 78 (1981).

19.   T. V. Hromadka, II and Chintu Lai, The Complex Variable Boundary Element Method in Eningeering Analysis, Springer-Verlag, NY, 28 (1987).

FIGURE CAPTIONS

Fig. 1   Schemastic Diagram of a two-dimensional craze

Fig. 2   Mesh division for viscoelastic infinite plate with a hole

Fig. 3   Radial displacement of viscoelastic infinite plate with a hole

Fig. 4   Mesh division for a quarter plate with a craze

Fig. 5   Creep opening displacement of the craze surface

Fig. 6   Comparison of stress distribution of craze surface in

time = 500 hours and time = 0.
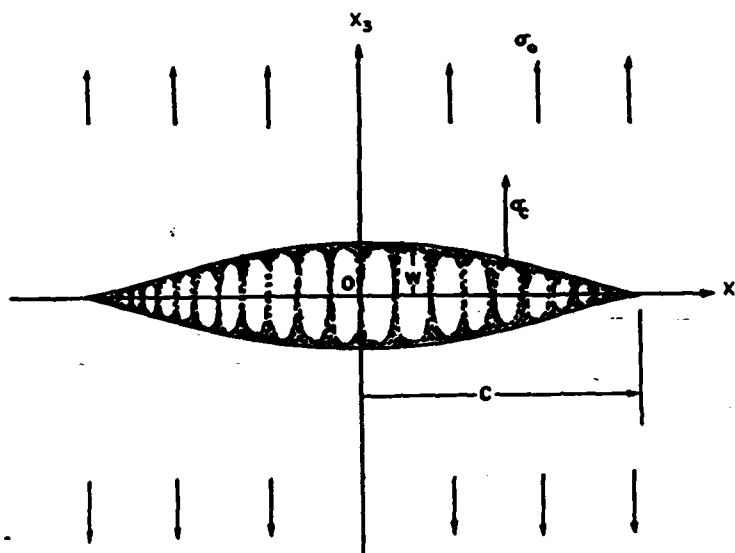
Fig. 1   Schematic Diagram of a two-dimensional craze
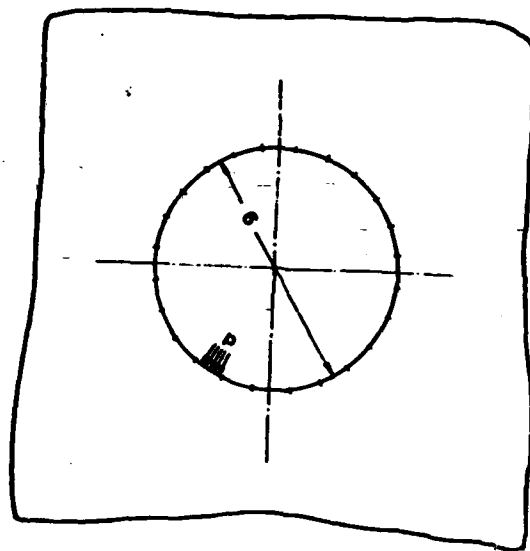
Fig. 2   Mesh division for viscoelastic infinite plate with a hole
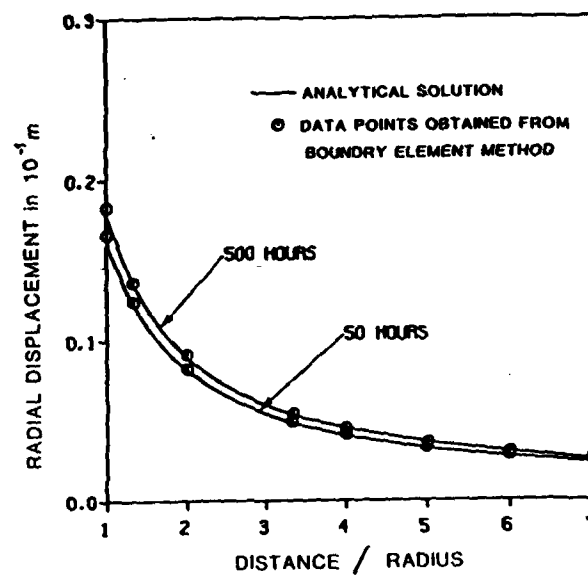
Fig. 3   Radial displacement of viscoelastic infinite plate with a hole
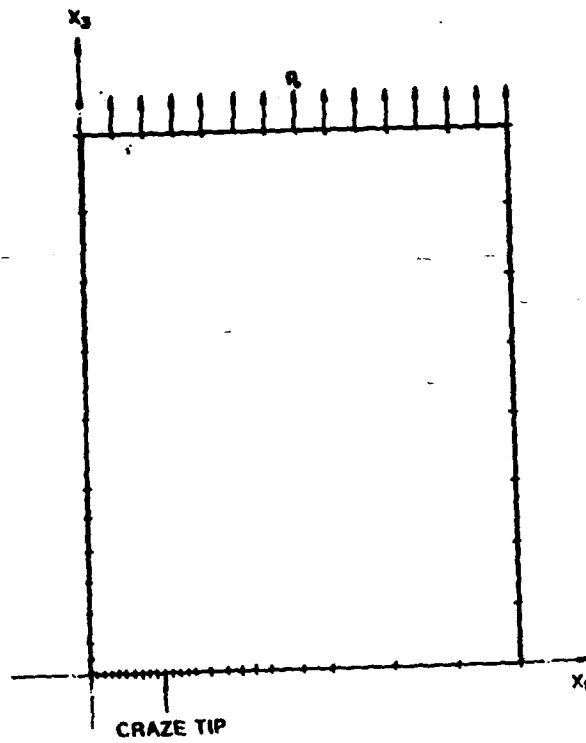
Fig. 4   Mesh division for a quarter plate with a craze

ANALYSIS OF CRACK-INDUCED-CRAZE IN POLYMERS

B.N.SUN, H.S.HOU AND C.C.HSIAO

DEPARTMENT OF AEROSPACE ENGINEERING & MECHANICS

UNIVERSITY OF MINNESOTA

MINNEAPOLIS, MINNESOTA 55455

ABSTRACT

In this paper, the viscoelastic boundary element method is used to estimate the opening displacement and the envelope stress on the surface of an isolated crack-induced-craze system. To predict the propagation history of both the crack and the craze in a polymer sheet, the material properties of the glassy polymers are represented by a generalized linear viscoelastic model. In the calculation, the energy absorption criterion is utilized to determine the initial breaking time and the propagation rate. A sequence of numerical calculations of crack-induced-craze propagation by means of the boundary element method are carried out. Results are compared with the theoretical micromechanics predictions. Good agreements are obtained. This investigation illustrates that the three-step envelope stress profile is resonably adequate for use in analyzing polymer quasifracture problems. The stress concentration phenomenon, neglected on the Dugdale-model, is taken into consideration in the present work.

INTRODUCTION

The quasifracture and fracture behaviors of a crack-induced-craze system in glassy polymers have been investigated extensively by many researchers both theoretically and experimentally up to now[1-8]. Generally speaking, the crack-induced-craze model in micromechanics accentuats the opening displacement, the envelope stress distribution around the interfaces of a craze, and especially the propagation processes of the craze and the crack. For some of the studies[5-7] the opening displacement profile has been determined experimentally first, from which the envelope stress destribution was evaluated by some analytical methods such as Fourier transform. Whereas others obtain the envelope stresses based upon experimental observations first, then the opening displacement profile analytically. Some scientists[6,9] considered that the yield property beyond the crack tip would determine the cracking and crazing properties, thus Dugdale model was employed. Although Dugdale model is thought to be able to predict the overall effect, it is questionable whether it is good enough in representing the true behavior of cracking and crazing properties in glassy polymers. Based on a number of experimental observations and theoretical analyses[6,7], Hsiao et al proposed the stress step-distribution model some years ago[2], which seems more resonable and accurate in representing the properties of the region behind the craze tips.

Until now quite a lot of investigations on this subject matter have been reported, among which most were done by experimental or

analytical method. Papers using numerical methods for predicting the cracking and crazing behaviors have also appeared. L.Bevan[10,11] studied the craze micromechanics by using linear boundary element method, in which the craze at crack tip was modeled by linear springs with constant stiffness. However, the linear elasticity and constant stiffness are not accurate enough to represent the properties of crack-induced-craze system in glassy polymers since it is well known that glassy polymers behave viscoelastically rather than elastically, and the drawing process is the dominant mechanism in polymer crazing. Therefore, some scientists considered the time dependent crack-craze propagation, such as Chern and Hsiao[2], McCartney[12] and Schapery[13] who applied the linear viscoelastic model for studying the craze or crack propagation, and Schapery[14], also studied the crack growth in nonhomogeneous viscoelastic media for opening crack model. Some others[15,16] investigated the nonlinear quasifracture properties using finite element method, and the time-dependent behavior of a craze using viscoelastic boundary element method. In these studies, the polymer material around the crack or craze has been regarded as viscoelastic represented by a generalized Kelvin model. The relationship between the tractions and the displacement of fibril domains in a craze was represented by a convolution integral. Using the correspondence principle in linear viscoelasticity and the boundary element method, the time-dependent opening displacement field and the stress distribution along the craze surface envelope have been calculated numerically.

In this article, the viscoelastic boundary element method is utilized

3

to study the propagation of a crack-induced-craze system. Meanwhile, the opening displacement profile and the envelope stresses on the craze interface surface have been obtained for different propagation steps. For comparison, the theoretical analysis using energy balance method was formulated, with a three-step stress distribution for calculating the propagation of the crack-induced-craze system. And the opening displacement profile of the crack-craze contour was also evaluated. Because of the change of the boundary conditions during the propagation of both the craze and the crack, Salamon's[17] supperposition principle of a step-like propagation has been applied to this problem, and a numerical calculation sequence of the boundary element method has been derived. Comparing the numerical and analytical results, good agreement has been obtained. It appears that the step distribution of the envelope stress used in the analysis is a good approximation suitable in dealing with glassy polymers. The viscoelastic boundary element method has the advantage of ease in preliminary preparation, economical in computing time, and the required accuracy for studying the crack-induced-craze system propagation problem may be achieved without much difficulty.

THEORETICAL CONSIDERATIONS

Craze is filled with load bearing highly oriented fibril domains and cavitated networks formed by continuous flowing of the bulk polymer during the crazing process. Based upon some experimental observations [18,19] and the craze model developed earlier[2], referring to a central fixed (x_1, x_3) coordinate system, an idealized symmetric crack-induced craze system in a constant simple stress field σ_0 is shown in Fig.1. Fig.2 shows $c(t)$ as the half length of the crack-craze system and $a(t)$, the half length of the crack only at time t. The stresses acting on the interfaces are called the envelope stresses with notation $\sigma_c(x_1, t)$ as a function of position and time. The half distance $w(x_1, t)$ between two craze or crack interfaces is known as the half opening displacement.

The half opening displacement of the crack-induced-craze system in a viscoelastic polymeric sheet can be obtained by using the correspondence principle in linear viscoelasticity theory[20]. The field equations and the constitutive relations are:

$$\sigma_{ij,j}(x_1, x_3, t) = 0 , \tag{1}$$

$$\epsilon_{ij}(x_1, x_3, t) = \frac{1}{2}[U_{i,j}(x_1, x_3, t) + U_{j,i}(x_1, x_3, t)] , \tag{2}$$

$$e_{ij}(t) = \int_{-\infty}^{t} J_1(t-\tau)\frac{\partial S_{ij}(\tau)}{\partial \tau} d\tau , \tag{3}$$

$$\epsilon_{kk}(t) = \int_{-\infty}^{t} J_2(t-\tau)\frac{\partial \sigma_{kk}(\tau)}{\partial \tau} d\tau , \tag{4}$$

5

where σ_{ij} is the stress tensor, ε_{ij} the strain tensor, $U_{i,j}$ the displacement gradients, and J_1 and J_2 are respectively the shear and isotropic creep compliance functions of the original bulk medium.

$$S_{ij}(t) = \sigma_{ij}(t) - \frac{1}{3} \delta_{ij} \sigma_{kk}(t) , \qquad (5)$$

$$e_{ij}(t) = \varepsilon_{ij}(t) - \frac{1}{3} \delta_{ij} \varepsilon_{kk}(t) , \qquad (6)$$

with i,j and k=1,3 denoting dummy variables. The boundary conditions are,

$$\sigma_{31}(x_1,0,t) = 0 , \qquad\qquad |x_1| < c(t) , \qquad (7)$$

$$\sigma_{33}(x_1,0,t) = \sigma_c(x_1,t) , \qquad\qquad |x_1| < c(t) , \qquad (8)$$

$$\left.\begin{array}{l} \sigma_{33}(x_1,x_3,t) = \sigma_0(t) \\ \sigma_{11}(x_1,x_3,t) = 0 \\ \sigma_{13}(x_1,x_3,t) = 0 \end{array}\right\} \text{ as } (x_1{}^2 + x_3{}^2) \to \infty . \qquad \begin{array}{l} (9) \\ (10) \\ (11) \end{array}$$

The opening displacement $w_0(x_1,t)$ is defined as

$$w_0(x_1,t) = U_3(x_1,0,t) , \qquad\qquad |x_1| < c(t) . \qquad (12)$$

To solve this viscoelastic problem, the Laplace transform of the field equations and the boundary conditions is applied to reduce the time dependency. Then the solution to the transformed equations can be found by using Muskhelishvili's complex variable conformal mapping method[21] or Westergaard's complex variable stress function method[22] for elastic medium when $c(t)$, $a(t)$ and $\sigma_c(x,t)$ remain unchanged with respect to time[23].

The time dependent solution of the original problem is obtained by Laplace inversion. This solution is valid only if the boundary conditions

6

are independent of time as mentioned earlier. These shortcomings can be surmounted by using a superposition method, i.e. a sequence of loading and unloading steps[17,24], which yields,

$$w_0(x_1,t) = C_b(0)\,\Phi(x_1,t) + \int_0^t \dot{C}_b(t-\tau)\,\Phi(x_1,\tau)\,d\tau, \qquad (13)$$

where

$$\Phi(x_1,t) = \sigma_0\sqrt{c^2-x_1^2} - \frac{2}{\pi}\int_0^c \sigma_c(\eta,t)\,\ln(c+\sqrt{c^2-\eta^2})\,d\eta$$

$$+ \frac{2}{\pi}\int_0^{x_1}\sigma_c(\eta,t)\,\ln(x_1+\sqrt{x_1^2-\eta^2})\,d\eta + \frac{2}{\pi}\int_{x_1}^c \sigma_c(\eta,t)\,\ln\eta\,d\eta,\quad (14)$$

and with an assumed constant strain ratio v. L^{-1} being the Laplace inversion:

$$C_b(t) = L^{-1}\frac{2(1-s^2v^2)}{s^2\overline{E}}, \qquad (15)$$

where E is the relaxation modulus of the bulk polymer and $\overline{E}(s)$ represents the same in the Laplace domain s.

Taking into consideration of the thickness of the primordial layer from which the fibril domain structure has been pulled out, the actual opening displacement of the system becomes[25,26]:

$$w(x_1,t) = C_b(0)\,\Phi(x_1,t) + \int_0^t \dot{C}_b(t-\tau)\,\Phi(x_1,\tau)\,d\tau + \int_{t_{x_1}}^t \frac{\dot{w}(x_1,\tau)}{\lambda(x_1,\tau)}\,d\tau, \quad (16)$$

where t_{x_1} is the time when the crack-craze-system tip first-reaches the point x_1, and λ is the draw ratio. The values of λ are found to be virtually unchanged along the periphery of the craze[8,27-31], with only a

7

slightly increase in the central region and near the craze tip. Therefore, λ can be considered as a constant and the opening displacement reduces to:

$$w(x_1,t) = \frac{\lambda}{\lambda-1}[C_b(0)\,\Phi(x_1,t) + \int_0^t \dot{C}_b(t-\tau)\,\Phi(x_1,\tau)\,d\tau]\,,$$

$$\text{for } a(t) \leq x_1 \leq c(t)\,, \tag{17}$$

$$w(x_1,t) = C_b(0)\,\Phi(x_1,t) + \int_0^t \dot{C}_b(t-\tau)\,\Phi(x_1,\tau)\,d\tau + \frac{1}{\lambda}w(x_1,t_a)\,,$$

$$\text{for } 0 \leq x_1 \leq a(t)\,, \tag{18}$$

where t_a denotes the time when the crack tip arrives at the point $x_1=a$.

The crack and craze lengths can be obtained by considering the energy balance. The energy absorbed by the craze[32] is spent to nucleate fibril domains near the craze tips, to pull fibrils out of the craze envelope surfaceand to break the fibril boundles[4]. With the supposition that the fibril nucleation rate at the craze tips is proportional to the systrm growth velocity $\dot{c}(t)$[33], the energy rate necessary for craze tip growth is $\Gamma_c\dot{c}(t)$. Similarly, the energy rate required for the crack tip growth is $\Gamma_a\dot{a}(t)$, where Γ_c and Γ_a are material constants. Based upon the assumption that the energy rate required for drawing fibrils out of the craze envelope surface is proportional to the new fibril domain surface creation rate $\dot{S}(t)$, and use the proportionality constant Γ_s, we have the following local energy rate balance equation:

$$\dot{H}_c(t) = \Gamma_c\dot{c}(t) + \Gamma_a\dot{a}(t) + \Gamma_s\dot{S}(t) \tag{19}$$

8

where $H_c(t)$ is the energy absorption rate of the quadrantal system. Here the strain energy, energy dissipation and kinetic energy have been neglected since during steady state they are negligible compared with the other rate quantities. With this simplification and the terms defined earlier, it follows that[2,3,32-34]

$$\dot{H}_c(t) = \int_0^c \sigma_c(x_1,t) \frac{\partial w(x_1,t)}{\partial t} dx_1 , \tag{20}$$

$$\dot{S}(t) = \int_0^c 4 \frac{V_f(x_1,t)}{d(x_1,t)} \frac{\partial w(x_1,t)}{\partial t} dx_1 , \tag{21}$$

Substituting into (19) results in

$$\int_0^c (\sigma_c - 4 \frac{\Gamma_s V_f}{d}) \frac{\partial w(x_1,t)}{\partial t} dx_1 = \Gamma_c \dot{c} + \Gamma_a \dot{a} , \tag{22}$$

where V_f is the volume fraction of the crazed polymer and d is the diameter of the individual fiber domains.

BOUNDARY ELEMENT CALCULATION

The viscoelastic boundary element method is applied to a polymer sheet with an isolated crack-induced-craze centrally located. The sheet is subjected to a unit step tension stress $\sigma_0 H(t)$, where $H(t)$ is the unit step function of time t. The material properties of the bulk polymer around the crack-induced-craze system is considered to be linearly viscoelastic. The constitutive equation can be expressed by convolution integral equations (3) and (4). For a linear viscoelastic polymer, a very convenient expression for the creep compliance $J(t)$ is obtainable by using a generalized Kelvin model[2,35,36] composed of a seriers of Voigt elements as described below:

$$J(t) = J_0 + \sum_{i=1}^{n} J_i(1-e^{-\frac{t}{\tau_i}}),\tag{23}$$

where J_0 and J_i are constants and τ_i, retardation times. Since some experimental results[32] have shown that the strain ratio $\nu(t)$ remains virtually unchanged for long creep times, the viscoelastic relaxation modulus $E(t)$ can be shown to be of the following form:

$$E(t) = L^{-1}[\frac{1}{s^2\bar{J}(s)}] = L^{-1}[\frac{1}{s(J_0+\sum_{i=1}^{n} J_i\frac{1}{\tau_i s+1})}],\tag{24}$$

where the bar indicates Laplace transform and L^{-1}, Laplace inversion. Taking into consideration of the fibril structure of the craze beyond the crack tip, the two opposite interfaces of the craze region are connected by the fibrillar structure as shown in Fig.2, which is formed by a fibrillation process due to the advances of the crack. These connections

10

are capable of transmitting load and can sustain large deformations. The stress state of an individual fibril domain is considered as an uniaxial tension. The relationship between the traction $T_3(x_1,t)$ and the opening displacement $U_3(x_1,t)$ of the crack-induced-craze system can be shown as follows:

$$T_3(x_1,t) = -\int_{-\infty}^{t} K(x_1,t-\tau)\frac{\partial U_3(x_1,\tau)}{\partial \tau}\, d\tau$$

$$= K(x_1,0)U_3(x_1,t) + \int_0^t \dot{K}(x_1,t-\tau)U_3(x_1,\tau)\, d\tau , \qquad (25)$$

on $x_1 < c$ and $x_3 = 0$,

where $K(x_1,t)$ is the stiffness per unit area on the craze surface and $K(x_1,0)$, the initial value of $K(x_1,t)$ at x_1. Using the molecular orientation theory[16], the stiffness turns out to be:

$$K(x_1,t) = L^{-1}[\frac{K(x_1,0)\, J_0}{s^2 \bar{J}(s)}] . \qquad (26)$$

It should be noted that the drawing process is the main mechanism of craze thickening. Thus $K(x_1,t)$ here is not the stiffness in the usual sense. It must take the drawing process into consideration.

The traction $T_3(x_1,t)$ acting along the craze envelope becomes

$$T_3(x_1,t) = -L^{-1}[s K(x_1,s)\, U_3(x_1,s)] . \qquad (27)$$

Because of the symmetry of the problem, only a quarter of the uniform sheet of width B, length L is considered in the boundary element calculation. The boundary conditions around the quadrantal sheet with isolated crack-induced-craze system are:

11

$$\begin{cases} T_3(x_1,t) = 0 , \\ T_1(x_1,t) = 0 , \end{cases} \qquad 0 \le x_1 \le a(t), \; x_3=0, \qquad (28)$$

$$\begin{cases} T_3(x_1,t) = -\int_0^t K(x_1,t-\tau)\dfrac{\partial U_3(x_1,\tau)}{\partial \tau}\, d\tau , \\ T_1(x_1,t) = 0 , \end{cases} \qquad a(t) \le x_1 \le c(t), \; x_3=0, \qquad (29)$$

$$\begin{cases} U_3(x_1,t) = 0 , \\ T_1(x_1,t) = 0 , \end{cases} \qquad c(t) < x_1 \le B, \; x_3=0, \qquad (30)$$

$$\begin{cases} T_1(x_1,t) = 0 , \\ T_3(x_3,t) = 0 , \end{cases} \qquad x_1=B, \; 0 \le x_3 \le L, \qquad (31)$$

$$\begin{cases} T_1(x_1,t) = 0 , \\ T_3(x_1,t) = \sigma_0 H(t) , \end{cases} \qquad 0 \le x_1 \le B, \; x_3=L, \qquad (32)$$

$$\begin{cases} U_1(x_3,t) = 0 , \\ T_3(x_3,t) = 0 , \end{cases} \qquad x_1=0, \; 0 \le x_3 \le L. \qquad (33)$$

As the crack-craze system propagates, new crack and craze surfaces are created. The associated energy release rate is

$$\dot{D}(t) = \Gamma_a \dot{a}(t) + \Gamma_c \dot{c}(t) . \qquad (34)$$

where Γ_a and Γ_c represent respectively the coefficients of fracture work for crack and the crack-induced-craze, and $a(t)$ and $c(t)$ are respectively the crack and the system propagation rates. The energy absorption rate for the crack-induced-craze system is expressed by Eq. (19). The energy absorption criterion claims that

$$\dot{D}(t) = \dot{H}_c(t) ,$$

i.e. $\quad \Gamma_a \dot{a}(t) + \Gamma_c \dot{c}(t) = \int_a^c \sigma_c(x_1,t)\dfrac{\partial U_3(x_1,t)}{\partial t}\, dx_1 . \qquad (35)$

12

In addition, sometimes the constant crack opening displacement criterion can be used as the propagation criterion of the crack-induced-craze system. But these two criteria are the same if the deformation associated with the crack tip is fixed with respect to time, a situation which occurs when the applied stress is constant. Thus both the crack and the craze propagate at the same velocity[37]. In this case, the opening displacement of the crack-induced-craze system is of the form:

$$U_3(x_1, t) = f[x_1 - c(t)] . \tag{36}$$

which means that the shape of the crack and that of the craze are conserved during the propagation, i.e.

$$\frac{dU_3}{dt} = -\dot{c}(t) f'[x_1 - c(t)] . \tag{37}$$

If the envelope stress is considered as the following step functional distribution:

$$\sigma_c = \begin{cases} \alpha_1 \sigma_0 & a(t) \leq x_1 \leq b(t) , \\ \\ \alpha_2 \sigma_0 & b(t) < x_1 \leq c(t) , \end{cases} \tag{38}$$

where $c(t) - b(t)$ is a small quantity representing the stress growth at the craze tip, then in the analysis, the energy absorption criterion formula (35) will be:

$$\Gamma_a \dot{a}(t) + \Gamma_c \dot{c}(t) = \int_a^b \alpha_1 \sigma_0 \frac{\partial U_3}{\partial t} dx_1 + \int_b^c \alpha_2 \sigma_0 \frac{\partial U_3}{\partial t} dx_1 , \tag{39}$$

$$\Gamma_a + \Gamma_c = \sigma_0 [\alpha_1 U_3(a,t) - (\alpha_1 - \alpha_2) U_3(b,t)] . \tag{40}$$

where $U_3(a,t) = U_3(x_1, t)\big|_{x_1 = a}$ and $U_3(b,t) = U_3(x_1, t)\big|_{x_1 = b}$, are the opening displacements of the crack tip and the craze tip respectively.

13

Noting that $U_3(b,t) << U_3(a,t)$, Eq.(40) becomes:

$$U_3(a,t) = \frac{\Gamma_\theta + \Gamma_c}{\sigma_0 \alpha_1} \; , \tag{41}$$

which is the constant crack opening displacement criterion in linear fracture mechanics. Therefore, in the theoretical and numerical analyses of the propagation of crack-induced-craze system, either the energy absorption criterion or the crack opening displacement criterion may be applied to determine the propagation rates at different times.

The viscoelastic boundary element method for analyzing crack-induced-craze system in polymers has been described in detail in an earlier study[16]. Using the correspondence principle in linear viscoelasticity theory, a series of transformed simultaneous algebraic equations can be solved. The displacement U_k and traction T_k on the boundary involving the crack-craze surface can be obtained in the Laplace domain. Based upon Schapery's collection numerical method[38] for Laplace inversion, the components of the stress and displacement fields at any point can be represented for the fixed time t by the series:

$$F(t) = C_0 + C_1 t + \sum_{m=1}^{M} A_m e^{-b_m t} \; , \tag{42}$$

with C_0, C_1, A_m and b_m being constants. Taking the Laplace transformation of Eq. (42) and mutiplying by the transform parameter s yield:

$$s\bar{F}(s) = C_0 + \frac{C_1}{s} + \sum_{m=1}^{M} \frac{A_m}{1 + \frac{b_m}{s}} \; , \tag{43}$$

14

where F(s) designates the Laplace transform of a time function F(t). When time t goes to infinity the function F(t) should remain finite. Therefore the constant C_1 has to be chosen as zero. After a sequence of s_k (k=1,2, ... M+1) is selected, the constants C_0 and A_m's can be calculated by the viscoelastic boundary element method, and the opening displacement U_{3j} and the envelope stress T_{3j} on the jth boundary element of crack-craze system surface for time t become

$$U_{3j} = D_{0j} + \sum_{m=1}^{M} D_{mj} e^{-\alpha_m t} , \tag{44}$$

$$T_{3j} = G_{0j} + \sum_{m=1}^{M} G_{mj} e^{-\beta_m t} . \tag{45}$$

Substituting the above two equations into the energy absorption criterion (35) for fracture, the breaking or the initial propagation time t of the crack-craze system for discreted boundary elements will be of the form:

$$t_b = \frac{\ell_T(\Gamma_a + \Gamma_c)}{\sum_{j=1}^{N} (T_{3j} - 4\frac{V_f}{d_f})\frac{dU_{3j}}{dt}\ell_j} , \tag{46}$$

where ℓ_T is the length of the boundary element on the crack tip and ℓ_j the jth element length on the crack-craze system, U_{3j} and T_{3j} are respectively the displacement and the envelope stress on jth boundary element of the crack-craze system surface before propagation. After the commencement of the propagation of the crack-craze system, both the boundary shape and the boundary conditions will change as a function of time. Therefore, the numerical solutions U_{3j} and T_{3j} are not valid for

15

propagating crack- craze system because the linear viscoelastic correspondence principle can only be applied to the problem with time independent boundary conditions. These restrictions can be removed by a generalized method of superposition principle, which uses stepwise development boundary conditions formulized by Salamon[17]. This method is utilized here to deal with the changing boundary conditions. A time dependent function F(t) after n steps in the time interval $t_n < t < t_{n+1}$ may be expressed as follows:

$$F(t) = \sum_{i=1}^{N-1} \{ F_i[r_i,(t-t_i)] - F_i[r_i,(t-t_{i+1})] \} + F_n[r_n,(t-t_n)] , \qquad (47)$$

where r_i is some critical linear dimension and F the solution, i.e. the opening displacement or the traction, which can be solved by the linear viscoelastic correspondence principle in the ith time step, t_n and t_{n+1} are the nth and the (n+1)th time steps. Similarly, the envelope traction T_{3j} and the displacement U_{3j} on jth element of the crack-craze system after the nth element propagates can be writen as:

$$U_{3j}^{(n)} = \sum_{i=1}^{M} D_{ij}^{(1)} \ (e^{-\alpha_i t_1} -1) \ e^{-\alpha_i(t_2+t_3+ \cdots +t_n)}$$

$$+ \sum_{i=1}^{M} D_{ij}^{(2)} \ (e^{-\alpha_i t_2} -1) \ e^{-\alpha_i(t_3+t_4+ \cdots +t_n)} + \cdots \cdots$$

$$+ \sum_{i=1}^{M} D_{ij}^{(n-1)} \ (e^{-\alpha_i t_{n-1}} -1) \ e^{-\alpha_i t_n}$$

$$+ \sum_{i=1}^{M} D_{ij}^{(n)} \ e^{-\alpha_i t_n} + D_{0j}^{(n)} \ , \qquad (48)$$

16

$$T_{3j}^{(n)} = \sum_{i=1}^{M} G_{ij}^{(1)} \, (e^{-\beta_i t_1} - 1) \, e^{-\beta_i (t_2 + t_3 + \cdots + t_n)}$$

$$+ \sum_{i=1}^{M} G_{ij}^{(2)} \, (e^{-\beta_i t_2} - 1) \, e^{-\beta_i (t_3 + t_4 + \cdots + t_n)} \quad + \cdots \cdots$$

$$+ \sum_{i=1}^{M} G_{ij}^{(n-1)} \, (e^{-\beta_i t_{n-1}} - 1) \, e^{-\beta_i t_n}$$

$$+ \sum_{i=1}^{M} G_{ij}^{(n)} \, e^{-\beta_i t_n} + G_{0j}^{(n)} \quad . \tag{49}$$

According to the principle, the calculation procedures are expounded as follows. The first step is to calculate the coefficients D_{ij} and G_{ij} on the jth element using the viscoelastic boundary element method, in which the length of crack is a_1 and that of the crack-craze system c_1. Then substituting D_{ij} and G_{ij} $(i=0,1,\ldots M)$ into Equation (35) the transition or the initial breaking time can be obtained. After that, both crack and craze propagate a distance of one element length for the steady state propagation case. Correspondingly the boundary conditions on the craze surface will shift forward by a length of one element. The second step is the calculation of D_{ij} and G_{ij} $(i=0,1,\ldots M)$ on the jth element using the same viscoelastic boundary element method. But at this time the length of crack is $a_1 + \ell$ and that of system $c_1 + \ell$, where ℓ is the length of an element. Substituting these coefficients, together with D_{ij} and G_{ij}, into Equations (25) and (26), the opening displacement U_{3j} of the system surface, the envelope traction Γ_{3j} can be obtained.

17

The breaking time t for the system to propagate to the next element can again be calaulated from the energy absorption criterion Equation (35). The same procedure continues to be iterated until the system grows to the nth element. At that time, the coefficients D_{ij} and G_{ij} are evaluated. And the opening displacement U_{3j} and the envelope stress T_{3j} on the jth element can be obtained at time t_n.

RESULTS

A quarter of the sheet used in the calculation using the boundary element method has unit thickness, width B=500μm and length L=600μm. The initial lengths of the system and the craze are taken to be $c(0)=98$μm and $a(0)=38$μm respectively. The total number of the boundary elements is 155 with the smallest element of the length 4μm located on the craze surface. The mesh construction is shown in Fig.3, where the elements around the craze tip are drawn in an enlarged scale. The surface of the crack-induced-craze system is divided into 23 boundary elements. Beyond the craze tip there are 10 elements in 40μm span.

The viscoelastic material properties are represented by a generalized Kelvin model (23) with other material constants taken to be as follows:

$$n = 4 ,$$

$$J_0 = 4.17 \times 10^{-4} \text{ m}^2/\text{MN} ,$$

$$J_1 = 0.71 \times 10^{-4} \text{ m}^2/\text{MN} ,$$

$$J_2 = 0.62 \times 10^{-4} \text{ m}^2/\text{MN} ,$$

$$J_3 = 0.43 \times 10^{-4} \text{ m}^2/\text{MN} ,$$

$$J_4 = 0.31 \times 10^{-4} \text{ m}^2/\text{MN} ,$$

$$v = 0.3 ,$$

$$\tau_1 = 1.0 \text{ hr. },$$

$$\tau_2 = 10.0 \text{ hr. },$$

$$\tau_3 = 80.0 \text{ hr. },$$

$$\tau_4 = 110.0 \text{ hr. },$$

$$\Gamma_c = 0.3 \text{ J/m}^2 ,$$

19

$\Gamma_a = 2.72$ J/m^2 ,

$\alpha_1 = 1.21$,

$\alpha_2 = 2.58$.

The following quantities occuring in the calculations of theoretical method are also used[39-41] :

$\lambda = 2$,

$\Gamma_s = 0.231$ J/m^2 ,

$d = 4.4$ nm ,

which represent the properties of polycarbonate. The applied stress is $\sigma_0 = 37.4$ MN/m.

The first kind of calculation is based upon the stiffness distribution shown in Fig.4. Correspondingly, the instantaneous opening displacement of the crack-induced-craze system is plotted in Fig.5 against the distance measured from the center of crack. The data points indicating the experimental observations[6,8], triangles represent the theoretical solutions, and the solid curve is the result obtained by the boundary element method. Initially the distribution of the stress normal to the surface is shown in Fig.6.

When the applied constant stress σ_0 is maintained, the opening displacement of the system increases as a result of creep and the drawing of the fibril domains. According to the energy absorption criterion, the craze-crack transition time $t_b = t_1$ can be determined numerically. Then the crack-craze system propagates steadily and the case that the crack and the system have the same velocity[9] is considered here. During the calculation of the propagation rate the stiffness on the

20

craze surface is shifted stepwise by one element. Fig.7 shows the time dependent normalized lengths of the crack-induced-craze system, where the points are obtained by the boundary element method and the solid line is calculated by theoretical method. As can be seen from the figure, the propagation rate at the steady state is almost constant. After a certain period of time, both the crack and the system propagation rates increase drastically. The opening displacement profile of the crack-craze system as a function of time is shown in Fig.8. The opening displacement profiles at different times exhibit somewhat similar shape. Fig.9 shows the comparison between the results obtained by the boundary element method and the analytical results at time t=12.21 hours. A very good agreement is obtained. Fig.10 shows the envelope stress distribution in the craze region.

The closeness between the theoretical results and those obtained by the boundary element method in Figs. 5, 7 and 9 connotes that the boundary element results are generally in good agreement with the analytical results. The accuracy depends on the mesh construction and the type of element used. Constant elements used in the boundary element calculation procedure yield satisfactory results in this case. The use of higher order elements, such as first and second order elements, or much smaller elements would improve the accuracy. The stress distribution on the craze surface has almost the same shape and magnitude throughout the propagation. In fact, it has been suggested that the Dugdale model is not fully adequate for analysis in describing the craze envelope stress. Nevertheless, the analytical formulation

21

using, the three-step distribution function has been shown to be a resonable and good approximation for analyzing the isolated crack-craze system. As can be seen in Figs. 6 and 10, there is a deep stress minimum just behind the tip of the craze. This characteristic feature persisted during the course of this investigation. This is somewhat similar to the results obtained earlier using the finite element method. Two extreme values in the envelope stress distribution have occurred. Like in the present case a minimum envelope stress is located at some point behind the craze tip where the stiffness gradient changes sharply and a maximum one occurs at the tip. Both of these extremes have been obtained by either analytical or experimental methods.[1,2,42,43,44] It is hoped that this phenomenon will be studied further to acquire a better understanding of its behavior with respect to the crack-craze system.

REFERENCES

1   S.S.Chern and C.C.Hsiao, J.Appl.Phys., 52,5994(1981).

2   S.S.Chern and C.C.Hsiao, J.Appl.Phys., 53,6541(1982).

3   Z.D.Zhang, S.S.Chern and C.C.Hsiao, J.Appl.Phys., 54,5568(1983).

4   S.S.Chern and C.C.Hsiao, Proceedings of ICF6, New Delhi, India, 2603 (1984).

5   B.D.Lauterwasser and E.J.Kramer, Phil.Mag., A39,469(1979).

6   Wen-chou V.Wang and E.J.Kramer, J.Mater.Sci., 17,2013(1982).

7   E.H.Andrews, "Development in polymer fracture"-1, p78, Applied Science Publishers LTD, London(1979).

8   A.M.Donald and E.J.Kramer, J.Mater.Sci., 16,2977(1981).

9   Elio Passaglia, Polymer, 23,754(1982).

10   L.Bevan, J.Polym.Sci.Phys. 19,1759(1981).

11   Idem, J.Appl.Polym.Sci., 27,4263(1982).

12   L.N.McCartney, Int.J.Fract., 13,641(1977), 14, 547(1978)

13   R.A. Schapery, Int.J.Fract., 11,141,369,549(1975).

14   R.A.Schapery, Int.J.Fract., 14,293(1978).

15   B.N.Sun and C.C.Hsiao, J.Appl.Phys., 57,170(1985).

16   B.N.Sun and C.C.Hsiao, to be published.

17   M.D.G.Salamon, Advances in Rock Mechanics, Part B, (National academy of Science, 1974).

18 P.Beahan, M.Bevis and D.Hull, J.Mater.Sci., 8,162(1972).

19 X.C.Lu, C.G.Fan and T.Z.Qian, Proceedings of ICF Int. symposium on Fract. Mech. (Beijing), 1075(1983).

20 R.M.Christensen, Thoery of Viscoelasticity-An Introduction, (Academic, New York, 1971).

21 N.I.Muskhelishvili, Some Basic Problems of Mathematical Thoery of Elasticity (Noordhoff, Gromigen, The Netherlands, 1953), p.340.

22 H.M.Westergaard, J.Appl.Mech., 6,49(1939).

23 N.V.Heymans and J.C.Bauwens, J.Mater.Sci., 11,7(1976).

24 H.K.Mueller, Ph.D thesis, California Institute of Technology, June, 1968.

25 J.Murray and D.Hull, J.Mater.Sci., 6,1277(1971).

26 S.S.Chern, Univ. of Minn., Mpls, Minn., Ph.D thesis, Aug(1983).

27 A.M.Donald and E.J.Kramer, J.Polym.Sci.Phys., 20,1129(1982).

28 T.Chan, A.M.Donald and E.J.Kramer, J.Mater.Sci., 16,676(1981).

29 R.P.Kambour, J.Polym.Sci., Part A, 2,4165(1964).

30 H.G.Krenz, et al, J.Mater.Sci., 11,2198(1976).

31 E.J.Kramer, et al, J.Polym.Sci.Phys., 16,349(1978).

32 S.S.Pang, Z.D.Zhang, S.S.Chern and C.C.Hsiao, J.Polym.Sci.Phys., 23, 683(1985).

33 S.S.Chern and C.C.Hsiao, J.Appl.Phys., 53,6541(1982).

34 H.H.Kaush and M.Dettermaier, Polym.Bull., 3,565(1980).

35 A.J.Stavarman, F.Schwarzl, Die Physik der Hochpolymeren, (edited by H.A.Stuart), Springer, Berlin(1965).

36 Z.Rigbi, Appl.Polym.Symposia, No.5, 1(1967).

37   P,Trassaert, R.Schirrer, J.Mater.Sci., 18,3004(1983).

38   R.A.Schapery, U.S. National Congress of Appl. Mech., 1075(1961).

39   A.M.Donald and E.J.Kramer, J.Polym.Sci.Phys., 20,899(1982).

40   E.J.Kramer, Polym.Eng.Sci., 24,761(1984).

41   N.V.Heymans, Polym.Eng.Sci., 24,809(1984).

42   J.C. Newman, Jr. AIAA J. 13,1017(1975).

43   J.C. Newman, Jr. ASTM STP 56,637(1977).

44   E.J. Kramer, Advances in Polymer Science,52/53,Crazing in Polymers,1, Springer-Verlag, Berlin, Heidelberg(1983).

FIGURES

Fig.1 Schematic fibrillar structure of a two-dimensional crack-induced craze system.

Fig.2 A two-dimensional quadrantal crack-induced-craze system.

Fig.3 Boundary element mesh with craze tip shown in an enlarged scale.

Fig.4 Stiffness distribution in craze region.

Fig.5 Opening displacement profile of crack-craze system.

Fig.6 Initial envelope stress on surface of craze region.

Fig.7 Time dependent normalized length of crack-induced-craze system.

Fig.8 Opening displacement of crack-craze system at several time steps.

Fig.9 Comparison of opening displacements by boundary element method and theoretical analysis.

Fig.10 Envelope stress on craze surface at time=12.21 hours.

26

FIG.1

FIG.2

σ_0

CRACK TIP

CRAZE TIP

X_3

O

X_1

C

X_3

CRACK TIP

CRAZE TIP

O

X_1

C
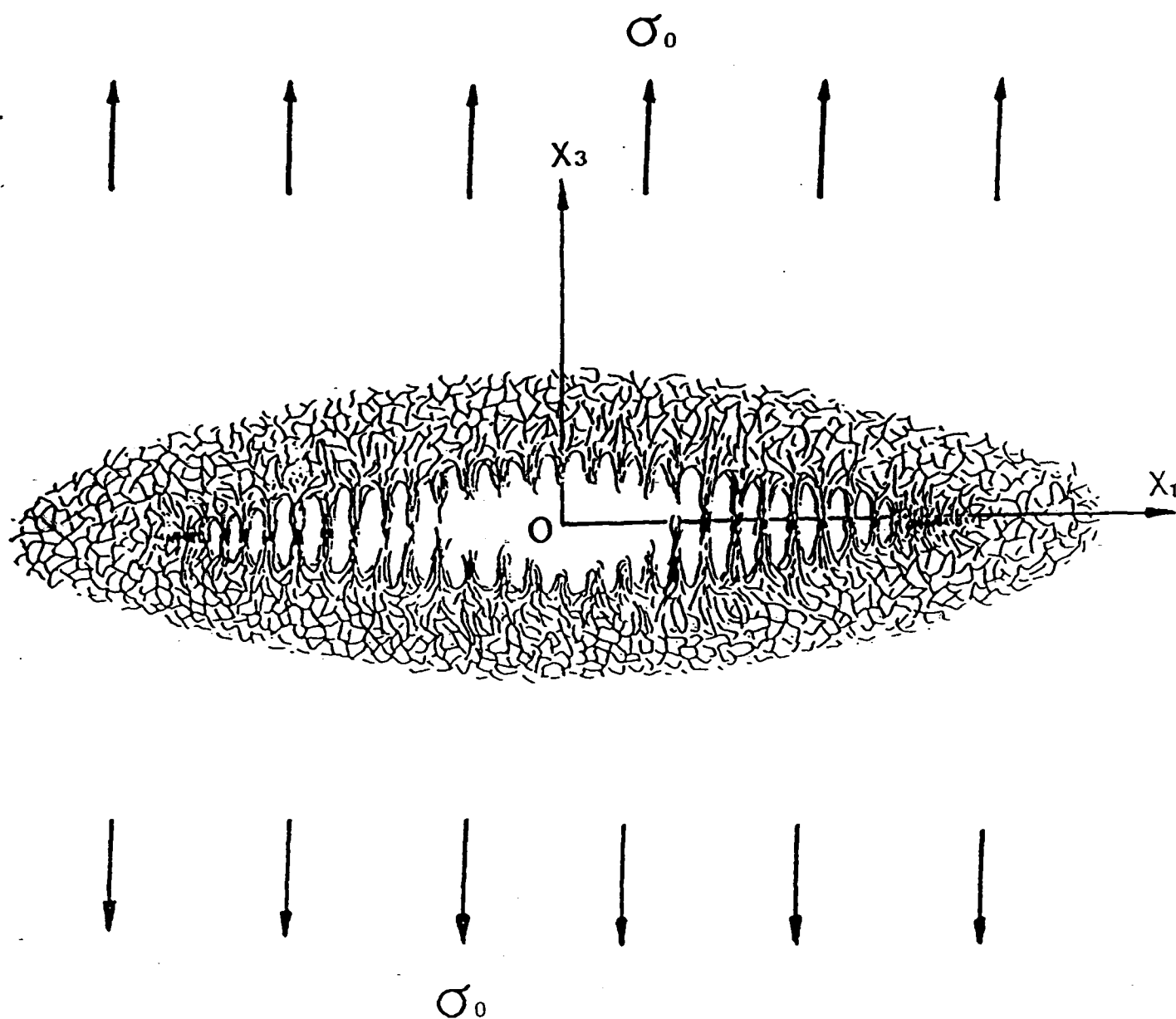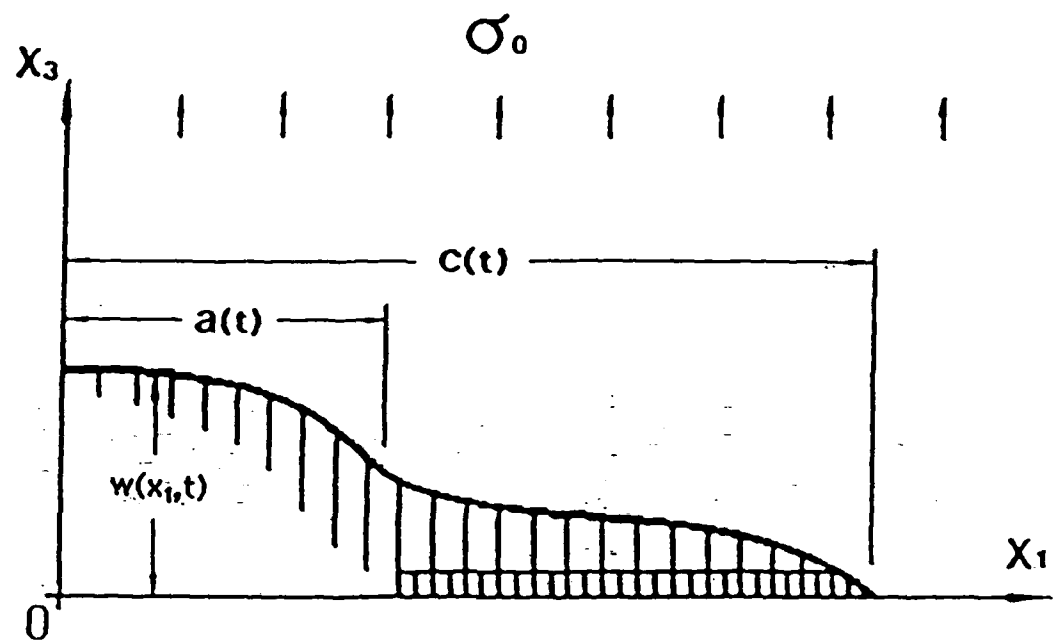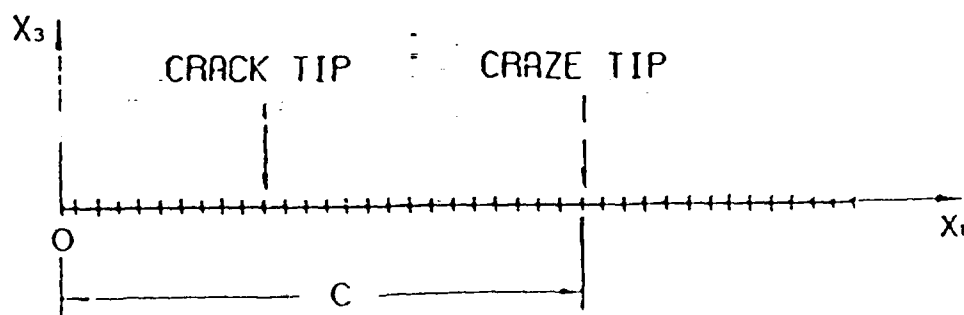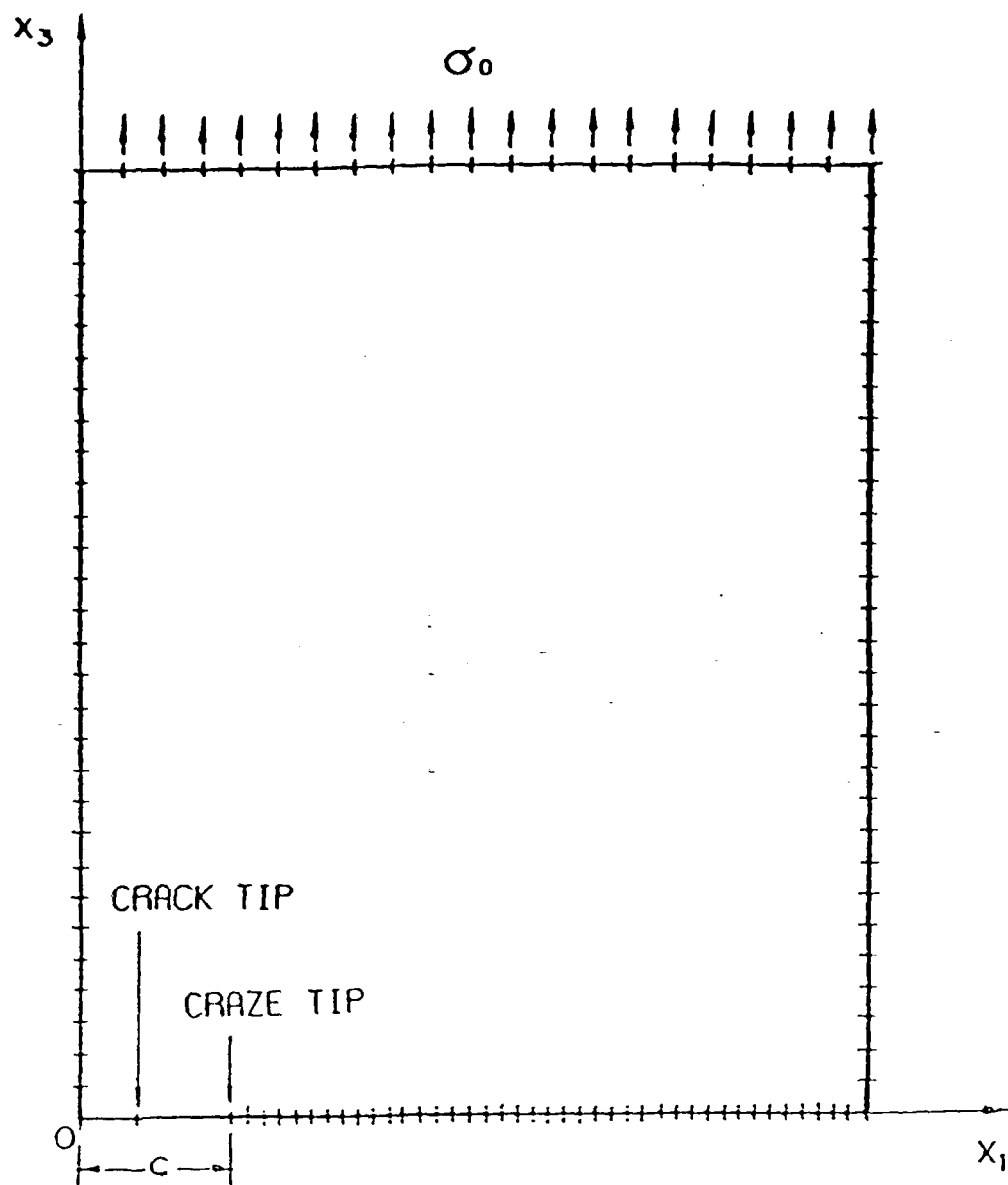
FIG.3
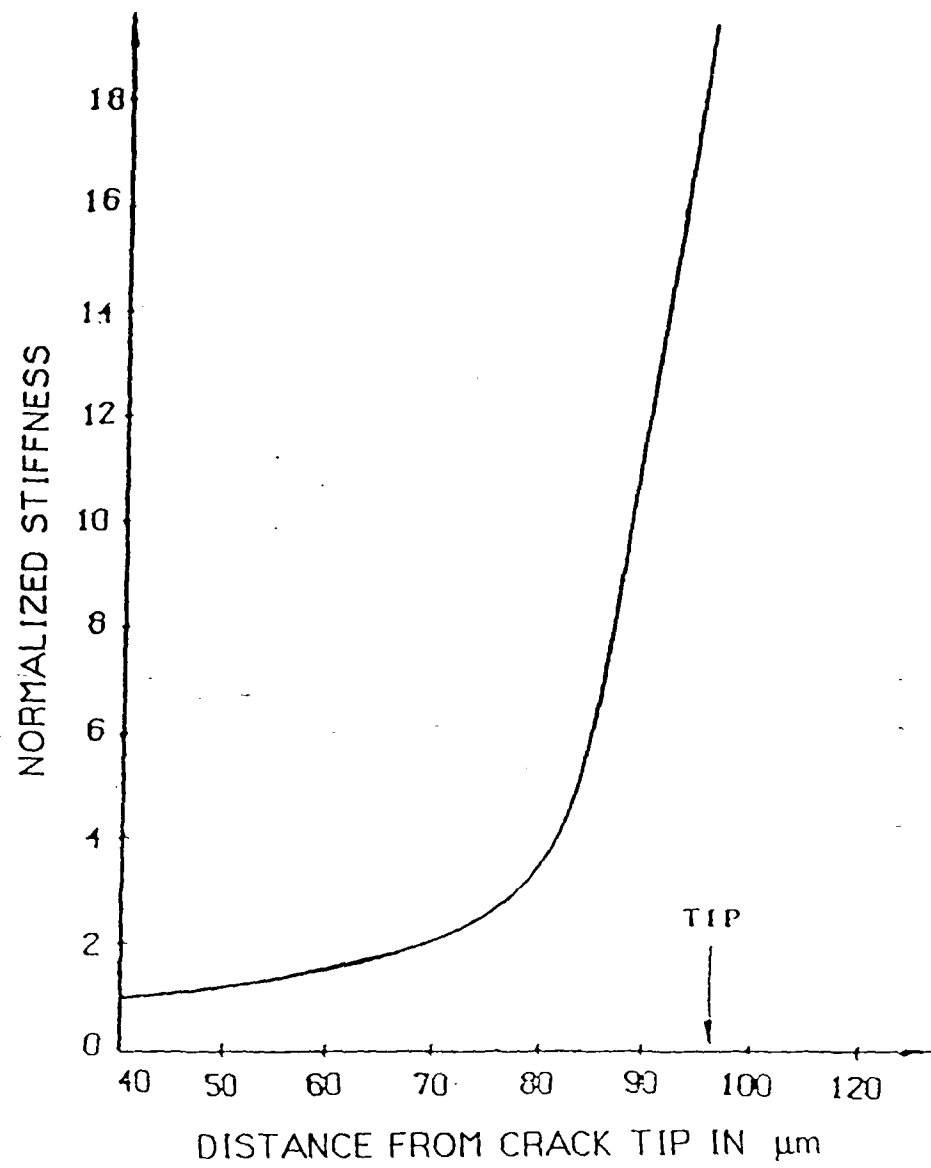
FIG.4
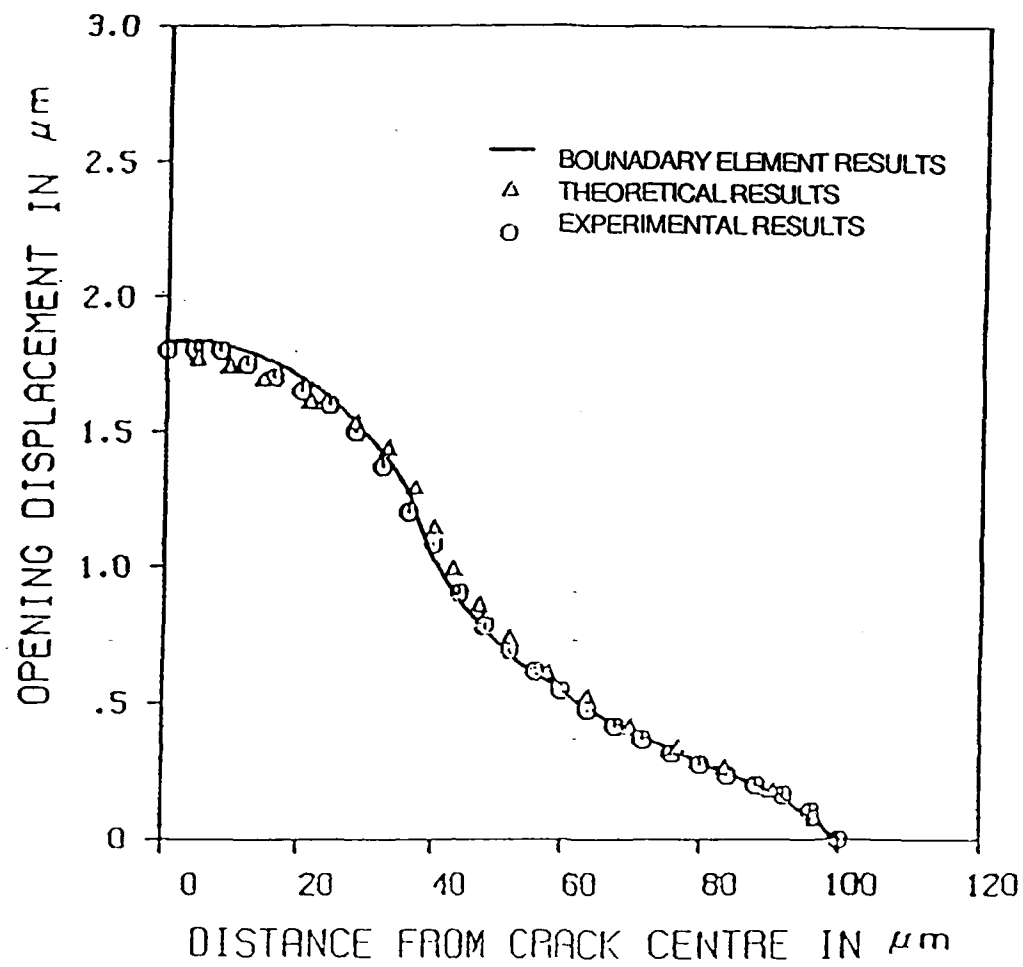
FIG.5
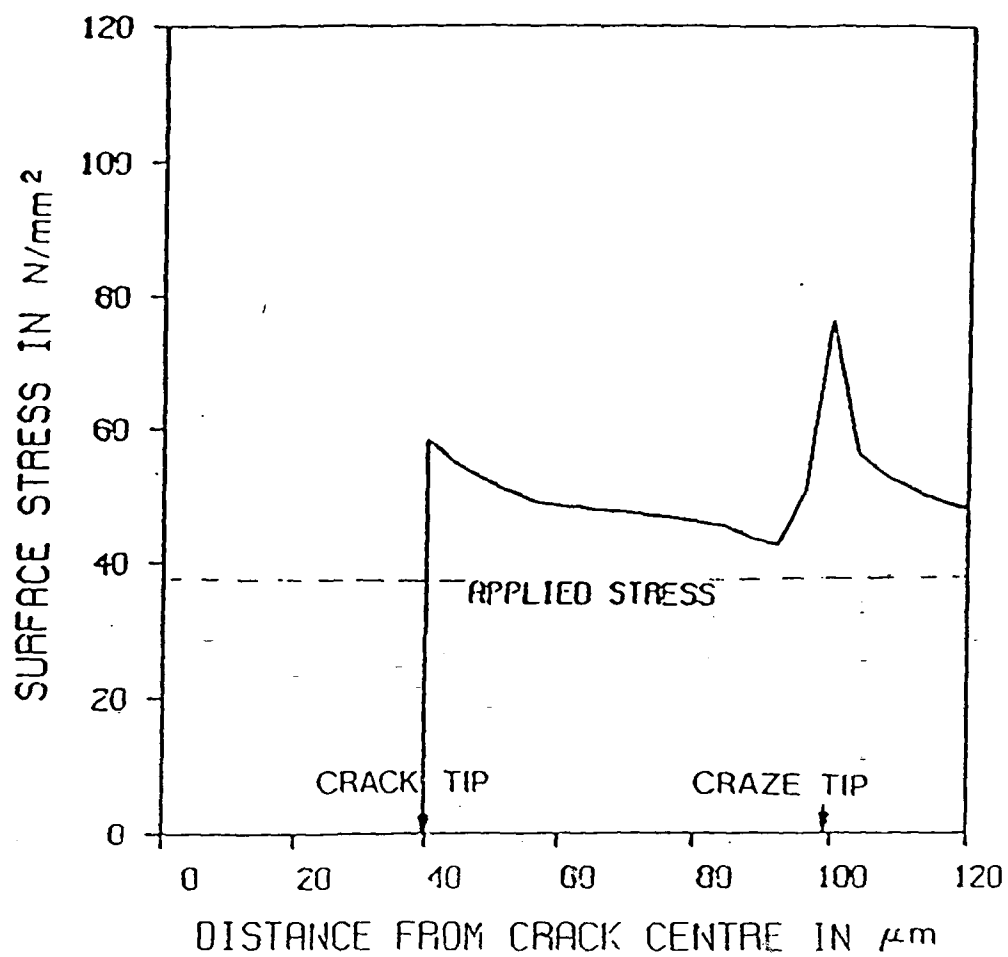
FIG.6

FIG.7

FIG.8

FIG.9

FIG.10